

Authors' Response

The authors would like to thank the Associate Editor for his further revision.

His comments and suggestions have improved the quality of the manuscript.

In the revised version, we have taken all of them into account and we have replied to his comments.

1 EPN-Repro2: A reference GNSS tropospheric dataset over Europe.

2 Rosa Pacione ⁽¹⁾, Andrzej Araszkiewicz ⁽²⁾, Elmar Brockmann ⁽³⁾, Jan Dousa ⁽⁴⁾

3 ⁽¹⁾ e-GEOS S.p.A, ASI/CGS, Italy

4 ⁽²⁾ Military University of Technology, Poland

5 ⁽³⁾ Swiss Federal Office of topography swisstopo

6 ⁽⁴⁾ New Technologies for the Information Society, Geodetic Observatory Pecný, RIGTC, Czech
7 Republic

8 *Correspondence to:* Rosa Pacione (rosa.pacione@e-geos.it)

9 **Abstract.** The present availability of 18+ years of GNSS data belonging to the EUREF Permanent
10 Network (EPN, <http://www.epncb.oma.be/>) is a valuable database for the development of a climate
11 data record of GNSS tropospheric products over Europe. This data record can be used as a reference
12 for a variety of scientific applications (e.g. validation of regional Numerical Weather Prediction
13 reanalyses and climate model simulations) and has a high potential for monitoring trends and the
14 variability in atmospheric water vapour. In the framework of the EPN-Repro2, the second
15 reprocessing campaign of the EPN, five Analysis Centres homogenously reprocessed the EPN
16 network for the period 1996-2014. A huge effort has been made for providing solutions that are the
17 basis for deriving new coordinates, velocities and tropospheric parameters for the entire EPN. The
18 individual contributions are then combined to provide the official EPN reprocessed products. This
19 paper is focused on the EPN-Repro2 tropospheric product. The combined product is described
20 along with its evaluation against radiosonde data and European Centre for Medium-Range Weather
21 Forecasts (ECMWF) reanalysis (ERA-Interim) data.

22 1. Introduction

23 The EUREF Permanent Network (Bruyninx et al., 2012; Ihde et al., 2013) is the key geodetic
24 infrastructure over Europe, currently made up by over 280 continuously operating GNSS reference
25 stations, and maintained on a voluntary basis by EUREF (International Association of Geodesy
26 Reference Frame Sub-Commission for Europe, <http://www.euref.eu>) members. Since 1996, GNSS
27 data collected at the EUREF Permanent Network have been routinely analysed by several (currently
28 16) EPN Analysis Centres (Bruyninx C. et al., 2015). For each EPN station, observation data along
29 with metadata information as well as precise coordinates and tropospheric Zenith Total Delay (ZTD)
30 parameters are publicly available. Since June 2001, the EPN Analysis Centres (AC) routinely
31 estimate ZTD in addition to station coordinates. The ZTD, available in daily SINEX TRO files, are
32 used by the coordinator of the EPN tropospheric product to generate each week the final EPN
33 solution containing the combined tropospheric estimates with an hourly sampling rate. The
34 coordinates, as a necessary part of this file, are taken from the EPN weekly combined SINEX file

Commentato [g1]: The acronym ZTD is having two different explanations here. Please be consistent and choose one.

Commentato [PR2R1]: We have chosen Zenith Total Delay

Commentato [g3]: See comment 1.

35 (<http://www.iers.org/IERS/EN/Organization/AnalysisCoordinator/SinexFormat/sinex.html>). Hence,
36 stations without estimated coordinates in the weekly SINEX file are not included in the combined
37 troposphere solution. The generation of the weekly combined products is done for the routine
38 analysis. Plots of the ZTD time series and ZTD monthly means as well as comparisons with respect
39 to radiosonde data are available in a dedicated section at the EPN Central Bureau web site
40 (http://www.epncb.oma.be/_productsservices/sitezenithpathdelays/). Radiosonde profiles are
41 provided by EUMETNET (European Meteorological Services Network) as an independent dataset
42 to validate GPS (NAVSTAR Global Positioning System) ZTD data, and are exchanged between
43 EUREF and EUMETNET for scientific purposes, based on a Memorandum of Understanding
44 between the two mentioned organisations ([http://www.euref.eu/documentation/MoU/EUREF-](http://www.euref.eu/documentation/MoU/EUREF-EUMETNET-MoU.pdf)
45 [EUMETNET-MoU.pdf](http://www.euref.eu/documentation/MoU/EUREF-EUMETNET-MoU.pdf)).

46 However, such time series are affected by inconsistencies due to updates of the reference frame and
47 the applied models, implementation of different mapping functions, use of different elevation cut-
48 off angles and any other updates in the processing strategies, that causes inhomogeneities over time.
49 To reduce processing-related inconsistencies, a homogenous reprocessing of the whole GNSS data
50 set is mandatory and, for doing it properly, a well-documented, long-term metadata set is required.

51 This paper focuses on the tropospheric products obtained in the framework of the second EPN
52 Reprocessing campaign (hereafter EPN-Repro2), for which, using the latest available models and
53 analysis strategy, GNSS data of the entire EPN network have been homogeneously reprocessed for
54 the period 1996-2014. The EPN homogeneous long-term GNSS time series can be used as a
55 reference dataset for a variety of scientific applications in meteorological and climate research.
56 Ground-based GNSS meteorology (Bevis et al., 1992) is very well established in Europe and dates
57 back to the 90s, starting with the EC 4th Framework Program (FP) projects WAVEFRONT (GPS
58 Water Vapour Experiment For Regional Operational Network Trials) and MAGIC (Meteorological
59 Applications of GPS Integrated Column Water Vapour Measurements in the western Mediterranean,
60 Haase et al., 2001). Early in this century, the ability to estimate ZTDs in Near Real Time has been
61 demonstrated (COST-716, 2005), and the EC 5th FP scientific project **TOUGH (Targeting Optimal**
62 **Use of GPS Humidity Measurements in Meteorology, 2003-2006)** was funded. Since 2005, the
63 operational production of tropospheric delays has been coordinated and monitored by the
64 EUMETNET GNSS Water Vapour Programme (E-GVAP, 2005-2017, Phase I, II and III,
65 <http://egvap.dmi.dk>). Guerova et al. (2016) report on the state-of-the-art and future prospects of the
66 ground-based GNSS meteorology in Europe. On the other hand, the use of ground-based GNSS
67 long-term data for climate research is still an emerging field.

Commentato [g4]: Add a date here.

Commentato [AA5R4]: Done, but Rosa please check it.

Commentato [PR6R4]: Checked, the time frame added is correct.

Promoting the use of reprocessed long-term GNSS-based tropospheric delay data sets for climate research is one of the objectives of the Working Group 3 ‘GNSS for climate monitoring’ of the EU COST Action ES 1206 ‘Advanced Global Navigation Satellite Systems tropospheric products for monitoring severe weather events and climate (GNSS4SWEC)’, launched for the period of 2013–2017. The Working Group 3 enforces the cooperation between geodesists and climatologists in order to generate recommendations on optimal GNSS reprocessing algorithms for climate applications, and to standardise for these applications the conversion method between propagation delay and atmospheric water vapour (Saastamoinen, 1973; Bevis et al., 1992; Bock et al. 2015). For climate applications, maintaining the long-term stability is a key issue. Steigenberger et al. (2007) found that the lack of consistencies over time due to changes in GNSS processing could cause inconsistencies of several millimetres in the GNSS-derived Integrated Water Vapour (IWV), making climate trend analysis very challenging. Jin et al. (2007) studied the seasonal variability of tropospheric GPS ZTD (1994-2006) over 150 international GPS stations and showed its relative trend in the northern and southern hemisphere as well as in coastal and inland areas. Wang and Zhang (2009) derived GPS Precipitable Water Vapour (PWV or PW) using the International GNSS Service (IGS, Dow et al., 2009) tropospheric products at about 400 global sites for the period 1997-2006 and analysed the PWV diurnal variations. Nilsson and Elgered (2008) reported on PWV changes from -0.2 mm to +1.0 mm in 10 years by using the data from 33 GPS stations located in Finland and Sweden. Sohn and Cho (2010) analysed the GPS Precipitable Water Vapour trend in South Korea for the period 2000-2009 and studied also the relationship between GPS PWV and temperature. A more thorough knowledge of atmospheric humidity, particularly in climate-sensitive regions, is essential to improve the diagnosis of global warming, and for the validation of climate predictions on which socio-economic response strategies. Suparta (2012) pointed out that the validation of PWV is an essential tool for solar-climate studies over a tropical region. Ning et al. (2013) used 14 years of GPS-derived IWV at 99 European sites to evaluate the regional Rossby Centre Atmospheric (RCA) climate model. GPS monthly mean data were compared against RCA simulations and ERA-Interim data. Averaged over the domain and the 14 years covered by the GPS data, they found IWV differences of about 0.47 kg/m² and 0.39 kg/m² for RCA-GPS and ERA-Interim-GPS, with standard deviations of 0.98 kg/m² and 0.35 kg/m², respectively. Alshawaf et al. (2017) found that GNSS IWV trends estimated at 113 GNSS sites in Europe, with 10 and 19 year temporal coverage, varies between -1.5 and 2 mm/decade with standard errors below 0.25 mm/decade. At these sites the ERA-Interim data analysed over 26 years show positive trends below 0.6 mm/decade, which correlate with the temperature trends.

101 Against this background, EPN-Repro2 is a unique dataset for the development of a climate data
102 records of GNSS tropospheric products over Europe, suitable for analysing climate trends and
103 variability, and calibrating/validating independent datasets at European and regional scales.
104 However, although homogeneously reprocessed, this time series still suffer from site-related
105 inhomogeneities due, for example, to instrumental changes (receivers, cables, antennas, and
106 radomes), changes in the station environment, etc. which might affect the analysis of the long-term
107 variability (Vey et al., 2009). Therefore, to get realistic and reliable water vapour trend estimates
108 such change points in the time series need to be detected and corrected for (Ning et al, 2016a).

109 This paper describes the EPN-Repro2 reprocessing campaign in Section 2. Section 3 is devoted to
110 the combined solutions, i.e. the official EPN-Repro2 products, while in Section 4 the combined
111 solution is evaluated w.r.t. radiosonde, ERA-Interim data and in terms of ZTD trends. The summary
112 and recommendations for future reprocessing campaigns are drawn in Section 5.

113 2. EPN second reprocessing campaign

114 EPN-Repro2 is the second EPN reprocessing campaign organized in the framework of the special
115 EUREF project “EPN reprocessing”. The first reprocessing campaign, which covered the period
116 1996-2006(Voelksen, 2011), involved the participation of all sixteen EPN Analysis Centres (ACs),
117 reprocessing their own EPN sub-network. This strategy guaranteed that each site was processed by
118 at least three ACs, which is an indispensable condition for providing a combined product. The
119 second reprocessing campaign covered all the EPN stations, which were operated from January
120 1996 through December 2013. Then, the participating ACs decided to extend this period until the
121 end of 2014 for tropospheric products. Data from about 280 stations in the EPN historical database
122 have been considered. As of December 2014, 23% of EPN stations are between 15-18 years old,
123 26% are between 10-14 years old, 30% between 5-10 years old, and 21% less than 5 years old. Only
124 five, over sixteen, EPN ACs (see [Table 1](#)) took part in EPN-Repro2, each providing at least
125 one reprocessed solution. One of the goals of the second reprocessing campaign was to test the
126 diversity of the processing methods in order to ensure the verification of the solutions. For this
127 reason, the three main GNSS software packages Bernese (Dach et al., 2014), GAMIT (King et al.,
128 2010) and GIPSY-OASIS II (Webb et al., 1997) have been used to reprocess the whole EPN
129 network and, in addition, several variants have been provided. In total, eight individual contributing
130 solutions, obtained using different software and settings, and covering different EPN networks, are
131 available. Among them, three are obtained with different softwares and cover the full EPN network,
132 while three are obtained using the same software (namely Bernese), but covering different EPN
133 networks. In [Table 2](#) the processing characteristics of each contributing solution are reported.

Formattato: Tipo di carattere: Non Corsivo, Controllo ortografia e grammatica

Formattato: Colore carattere: Testo 1, Inglese (Regno Unito)

Formattato: Tipo di carattere: Non Corsivo, Colore carattere: Testo 1, Inglese (Regno Unito)

134 Despite the software used and the analysed networks, there are few diversities among the provided
135 solutions, whose impact needs to be evaluated before performing the combination. In the
136 reprocessing campaign all the ACs used for the GNSS orbits the CODE (Center for Orbit
137 Determination in Europe) Repro2 product (Lutz et al., 2014), with one exception (see Table 2
138 2) where JPL (Jet Propulsion Laboratory) Repro2 products (Desai et al., 2014) are used. For
139 tropospheric modelling two mapping functions are used: GMF-Global Mapping Function (Boehm
140 et al., 2006a) and VMF1-Vienna Mapping Function (Boehm et al., 2006b), whose impact has been
141 evaluated in Tesmer et al., 2007.

142 **2.1 Impact of GLONASS data**

143 During the reprocessing period, the Russian satellite system GLONASS (Global'naja
144 Navigacionnaja Sputnikovaja Sistema) became operational, and GLONASS observations are
145 available since 2003. However, only from 2008 onwards the amount of GLONASS data (see Figure
146 1Figure 1) is significant. The impact of GLONASS observations has been evaluated in terms of raw
147 differences between ZTD estimates as well as on the estimated linear trend derived from the ZTD
148 time series. As a matter of fact, GPS data (from the American navigation satellite system) are used
149 by all ACs in this reprocessing campaign, while two of them (namely IGE and LPT) reprocessed
150 GPS and GLONASS observations. Two solutions were prepared and compared, using the same
151 software and the same processing characteristics, but different observation data: one with GPS and
152 GLONASS, and one with GPS data only. The difference in ZTD trends (Figure 2Figure 2) between
153 a GPS-only and a GPS+GLONASS solution shows no significant rates for more than 100 stations
154 (rates usually derived from more than 100000 ZTD differences). This indicates that the inclusion of
155 additional GLONASS observations in the GNSS processing has a neutral impact on the ZTD trend
156 analysis. Satellite constellations are continuously changing in time due to satellites being replaced
157 and newly added for all systems. For instance, in the near future the inclusion of additional Galileo
158 (navigation satellite system in Europe) and BeiDou (navigation satellite system in China) data will
159 become operational in the GNSS data processing. These data will certainly improve the quality of
160 the tropospheric products and our study here points out that the ZTD trends might be determined
161 independently of the satellite systems used in the processing, and therefore might not introduce
162 systematic changes in terms of ZTD trends.

163 **2.2 Impact of IGS type mean and EPN individual antenna calibration models**

164 According to the processing options listed in the EPN guidelines for the Analysis Centre
165 (http://www.epncb.oma.be/documentation/guidelines/guidelines_analysis_centres.pdf), EPN
166 individual antenna calibration models have to be used instead of IGS type mean calibration models,

Formattato: Colore carattere: Testo 1, Inglese (Regno Unito)

Formattato: Tipo di carattere: Non Corsivo, Colore carattere: Testo 1, Inglese (Regno Unito)

Commentato [g7]: Write out this acronym.

Commentato [AA8R7]: Done.

Commentato [g9]: Write out this acronym.

Commentato [AA10R9]: Done.

Formattato: Tipo di carattere: (asiatico) Times New Roman, Colore carattere: Nero

Formattato: Tipo di carattere: (asiatico) Times New Roman, Non Corsivo, Colore carattere: Nero, Controllo ortografia e grammatica

Formattato: Tipo di carattere: (asiatico) Times New Roman, Colore carattere: Nero

Formattato: Tipo di carattere: (asiatico) Times New Roman, Non Corsivo, Colore carattere: Nero, Controllo ortografia e grammatica

when available. Currently, individual antenna calibration models are available at about 70 EPN stations. As reported in [Table 2](#), there are individual solutions carried out with IGS type mean antenna calibration models only (Schmid et al., 2015) while others use IGS type mean plus EPN individual antenna calibration models. Therefore, for the same station, there are contributing solutions obtained applying different antenna models. To evaluate the impact of using these different antenna calibration models on the ZTD, two solutions were prepared and compared, using the same software and the same processing, but different antenna calibration models: the first solution used the IGS type mean models only, and the second one used the individual calibrations whenever it was possible and the IGS type mean for the rest of the antennas. An example of the time series of the ZTD differences obtained between applying ‘Individual’ and ‘Type Mean’ antenna calibration models for the EPN station KLOP (Kloppenheim, Frankfurt, Germany) is shown in [Figure 3](#). KLOP station is included in the EPN network since June, 2nd 2002, when a TRM29659.00 antenna from the Trimble Company with no radome was installed. In the forthcoming years, two major instrumentation changes occurred at the station: the first in June 27th 2007, when the previous antenna was replaced with a new type of Trimble antenna (TRM55971.00) and a dedicated hemisphere radome (TZGD) was installed, and a second change in June 28th 2013 with the installation of another type of Trimble antenna (TRM57971.00) and the same type of radome. For these three specific hardware sets the individual calibrations are available at the EPN Central Bureau (ftp://epncb.oma.be/pub/station/general/epnc_08.atx). Switching between phase centre corrections from type mean to individual (or vice versa) causes a disagreement in the estimated height of the stations, as was mentioned by Araszkiewicz and Voelksen (2016), and as a consequence in their ZTD time series. Depending on the antenna model, the offset at station KLOP in the up component (vertical displacement) is -5.2 ± 0.5 mm, 8.7 ± 0.6 mm and 5.6 ± 0.8 mm with a corresponding offset in the ZTD of 0.2 ± 0.5 mm, -1.5 ± 0.5 mm, -1.4 ± 0.8 mm, respectively. Similar values were obtained between solutions calculated for all stations/antennas for which individual calibration models are available. The corresponding offset in the ZTD has the opposite sign for the antennas with an offset in the up component larger than 5 mm (16 antennas) and, generally, does not exceed 2 mm. Such inconsistencies in the ZTD time series are not large enough to be captured during the combination process (see Section 3), where a 10 mm threshold in the ZTD bias (about 1.5 kg/m² IWV) is set in order to flag problematic ACs or stations.

2.3 Impact of non-tidal atmospheric loading

As reported in the International Earth Rotation and Reference Systems Service (IERS) Convention (2010), the diurnal heating of the atmosphere causes surface pressure oscillations with diurnal and

Formattato: Colore carattere: Testo 1, Inglese (Regno Unito)

Formattato: Tipo di carattere: Non Corsivo, Colore carattere: Testo 1, Inglese (Regno Unito)

Formattato: Tipo di carattere: Non Corsivo, Controllo ortografia e grammatica

Commentato [g11]: Add a bookmark here explaining that TRM55971.00 points to the provider and the type of the antenna. Similar for TZGD radome.

Commentato [AA12R11]: Done.

Commentato [g13]: Another TZGD radome?

200 semidiurnal variability and even higher harmonics. These atmospheric tides induce periodic
201 motions of the Earth's surface (Petrov and Boy, 2004). The conventional recommendation is to
202 calculate the station displacement using the Ray and Ponte (2003) tidal model. However, crustal
203 motion related to non-tidal atmospheric loading has been detected in station position time series
204 from space geodetic techniques (van Dam et al., 1994; Magiarotti et al., 2001, Tregoning and Van
205 Dam, 2005). Several models of station displacements related to this effect are currently available.
206 Non-tidal atmospheric loading models are not yet considered as Class-1 models by the IERS (IERS
207 2010), indicating that there are currently no standard recommendations for data reduction. To
208 evaluate their impact, two solutions, one with and one without a non-tidal atmospheric loading
209 model, have been compared for the year 2013. In the solution with the model, the National Centers
210 for Environmental Prediction (NCEP) model is used at the observation level during data reduction
211 (Tregoning and Watson, 2009).

212 Dach et al. (2010) have already found that the repeatability of the station coordinates improves by
213 20% when applying the non-tidal atmospheric loading correction directly on the data analysis and
214 by 10% when applying a post-processing correction to the resulting weekly coordinates. However,
215 the effect on the ZTDs seems to be negligible. Generally, it causes a difference below 0.5 mm with
216 a standard deviation not larger than 0.3 mm. The difference is thus below the level of confidence.

217 Figure 4 shows time series of the differences of the ZTDs and the up components between
218 two solutions obtained with and without non-tidal atmospheric loading for two EPN stations: KIR0
219 (Kiruna, Sweden) and RIGA (Riga, Latvia). Furthermore, there is no correlation between the values
220 of estimated differences and vertical displacements caused by non-tidal atmospheric loading, as
221 correlation coefficients for the analysed EPN stations were below 0.2.

222 3. EPN-Repro2 combined solutions

223 The EPN ZTD combined product is obtained applying a generalized least square approach
224 following the scheme described in Pacione et al. (2011). The first step in the combination process is
225 the reading and checking of the SINEX TRO files delivered by the ACs. At this stage, gross errors
226 (i.e. ZTD estimates with formal standard deviations larger than 15 mm) are detected and removed.
227 The combination starts if at least three different solutions are available for a single site. Then, a first
228 combination is performed to compute proper weights for each contributing solution, to be used in
229 the final combination step. In this last step the combined ZTD estimates, their standard deviations
230 and site/AC specific biases are determined. The combination fails if, after the first or second
231 combination level, the number of ACs becomes less than three. Finally, ZTD site/AC specific
232 biases exceeding 10 mm are investigated as potential outliers.

Formattato: Tipo di carattere: (asiatico) Times New Roman, Colore carattere: Nero

Formattato: Tipo di carattere: (asiatico) Times New Roman, Non Corsivo, Colore carattere: Nero, Controllo ortografia e grammatica

233 The EPN-Repro2 combination activities were carried out in two steps. First, a preliminary
 234 combined solution for the period 1996-2014 was performed taken all the available eight
 235 homogeneously reprocessed solutions (see [Table 2Table-2](#)) as input. The aim of this preliminary
 236 combined solution is to assess each contributing solution and to investigate site/AC specific biases
 237 prior to the final combination, flag the outliers and send feedback to the ACs. The agreement of
 238 each contributing solution w.r.t. the preliminary combination is given in terms of bias and standard
 239 deviation (not shown). The standard deviation is generally below 2.5 mm, with a clear seasonal
 240 behaviour (larger for larger ZTD values), while the bias is generally in the range of +/- 2 mm.
 241 However, there are several GPS weeks for which the bias and standard deviation exceeded the afore
 242 mentioned limits. To investigate these outliers, the time series of site/AC specific biases have been
 243 studied, since this analysis might be a useful tool to detect bad data periods and provide useful
 244 information for cleaning the EPN historical archive. An example is given in [Figure 5Figure-5](#) for
 245 the station VENE (Venice, Italy) for three contributing solutions AS0, GO4 and MU2 (G00 and
 246 GO1 are not shown but are very close to GO4). In the first years of the acquisition, the station
 247 VENE experienced tracking issues, clearly mirrored in both the bias and standard deviation time
 248 series.

249 All the site/AC specific biases are divided into three groups: the red group contains site/AC specific
 250 biases with values larger than 25 mm, the orange group contains site/AC specific biases in the range
 251 of [15 mm, 25 mm] and the yellow group contains site/AC specific biases in the range of [10 mm,
 252 15 mm]. In [Table 3Table-3](#) the percentages of red, orange and yellow biases for each contributing
 253 solution are summarized. The majority of biases belong to the yellow group; the percentage of
 254 biases in the orange group ranges from 12% for LP0 and LP1 solutions to 27% for the AS0 solution,
 255 while the percentage of biases in the red group ranges from 3% for the MU4 solution to 22% for the
 256 IG0 solution.

257 The final EPN-Repro2 tropospheric combination is based on the following input solutions: AS0,
 258 GO4, IG0, LP1 and MU2. MUT AC provided the MU2 solution after the preliminary combination,
 259 its only difference with respect to MU4 is the use of type mean antenna and individual calibration
 260 models, whose effect has already been described in section 2.2. For those AC providing more than
 261 one solution, we have chosen that carried out with the Vienna Mapping Function. The agreement in
 262 terms of bias and standard deviation of each contributing solution w.r.t. the final combination is
 263 shown in [Figure 6Figure-6](#). The standard deviation had improved significantly with respect to the
 264 preliminary combination (not shown here), due to the removal of outliers detected during this early
 265 combination. The standard deviation is below 3 mm before GPS week 1055 and 2 mm thereafter.

Formattato: Tipo di carattere: Non Corsivo, Controllo ortografia e grammatica

Commentato [g14]: I assume?

Commentato [PR15R14]: Yes

Formattato: Tipo di carattere: Non Corsivo, Controllo ortografia e grammatica

Commentato [g16]: I assume?

Commentato [PR17R16]: Yes

Formattato: Tipo di carattere: (asiatico) Times New Roman, Colore carattere: Nero, Inglese (Regno Unito)

Formattato: Tipo di carattere: (asiatico) Times New Roman, Non Corsivo, Colore carattere: Nero, Inglese (Regno Unito), Controllo ortografia e grammatica

Commentato [g18]: On which grounds? Please comment!

Commentato [PR19R18]: Added

Formattato: Tipo di carattere: (asiatico) Times New Roman, Colore carattere: Nero

Formattato: Tipo di carattere: (asiatico) Times New Roman, Non Corsivo, Colore carattere: Nero, Controllo ortografia e grammatica

266 This is related to the worse quality of data and products during the first years of the EPN/IGS
267 activities.

268 The final EPN-Repro2 tropospheric combination is consistent with the final coordinate combination
269 performed by the EPN Analysis Centre Coordinator. During the coordinate combination all stations
270 were analyzed by comparing their coordinates for specific ACs and the preliminary combined
271 values. In the cases where the differences were larger than 16 mm in the up component (vertical
272 displacement), the station was eliminated and the whole combination process was repeated, up to
273 three times, if necessary. This ensures the consistency of the individual contributing solution w.r.t.
274 the final coordinates at the level of 16 mm in the up component. As internal quality metric, we have
275 considered the site coordinate repeatability of the final coordinate combination (Figure 7Figure 7).
276 As a rule of thumb, 9 mm repeatability in the up component (i.e. 3 mm in ZTD as explained in
277 Santerre, 1991) are needed to fulfill the requirement of retrieving IWV at an accuracy level of 0.5
278 kg/m2 (Bevis et al., 1994; Ning et al., 2016b). As shown in Figure 7Figure 7, only at one site,
279 MOPI (Modra Piesok, Slovakia), this threshold is exceeded on the long term. As reported at the
280 EPN Central Bureau, MOPI has been excluded several times from the routine combined solutions
281 because it has very bad observation periods in the past due to a radome manipulation that caused
282 jumps in the height component. However, this 9mm threshold has been temporary exceeded at
283 several stations during bad periods, an example is given in Figure 8Figure 8 for VENE (Venezia,
284 Italy).

285 4. Evaluation of the ZTD Combined Products with respect to independent data sets

286 The evaluation with respect to other sources or products, such as radiosonde data from the E-GVAP
287 and numerical weather re-analysis from the European Centre for Medium-Range Weather Forecasts,
288 ECMWF (ERA-Interim), provides a measure of the accuracy of the ZTD combined products.

289 4.1 Evaluation versus radiosonde

290 For the GPS and radiosonde (RS) comparisons at the EPN collocated sites, we used profiles from
291 the World Meteorological Organization (WMO) provided by EUMETNET in the framework of the
292 Memorandum of Understanding between EUREF and EUMETNET. Radiosonde profiles are
293 processed using a software by Haase et al. (2003) that checks the quality of the profiles, converts
294 the dew point temperature to specific humidity, shifts the radiosonde profile to correct for the
295 altitude offset between the GPS and the radiosonde sites, and determines the ZTD and IWV
296 compensating for the change of the gravitational acceleration g with height.

297 A comparison of the GNSS and radiosonde ZTD time series for the EPN site CAGL (Cagliari,
298 Sardinia Island, Italy) is shown in Figure 9Figure 9, with the mean biases and standard deviations

Formattato: Tipo di carattere: (asiatico) Times New Roman, Colore carattere: Nero

Commentato [g20]: So, it turns out that the threshold is 9 mm in the up comment (see also Fig. 7). So, why are so speaking about this 16mm differences in the up component? This is totally not clear to me. Please explain.

Commentato [PR21R20]: 16 mm is the threshold in the up component used by the EPN ACC when combining site coordinates.
http://www.epnacc.wat.edu.pl/storage/comb_strateg.pdf
While 9 mm is the repeatability considered as internal quality metric.
Hope it is now clear.

Formattato: Tipo di carattere: (asiatico) Times New Roman, Colore carattere: Nero

Formattato: Tipo di carattere: (asiatico) Times New Roman, Colore carattere: Nero

Formattato: Tipo di carattere: (asiatico) Times New Roman, Non Corsivo, Colore carattere: Nero, Controllo ortografia e grammatica

Formattato: Tipo di carattere: (asiatico) Times New Roman, Colore carattere: Nero, Inglese (Regno Unito)

Formattato: Tipo di carattere: (asiatico) Times New Roman, Non Corsivo, Colore carattere: Nero, Inglese (Regno Unito), Controllo ortografia e grammatica

299 reported in the Figure. Similarly, we computed an overall bias (RS minus GNSS) and standard
300 deviation for all the 183 EPN collocated sites, using all the data available in the considered period
301 (Figure 10). In this figure, the sites are sorted with increasing distance from the nearest
302 radiosonde launch site. For instance, MALL (Palma de Mallorca, Spain) is the closest (0.5 km to the
303 radiosonde site with WMO code 8301) while GRAZ (Graz, Austria) is the most distant (133 km to
304 RS WMO code 14015). The amount of data available for the comparisons varies between sites,
305 depending on the availability of the GPS and radiosonde ZTD estimates in the considered epoch,
306 and ranges from 121 pairs for VIS6 (Visby, Sweden, integrated in the EPN since 22-06-2014) up to
307 21226 pairs for GOPE (Ondrejov, Czech Republic, integrated in the EPN since 31-12-1995).

308 The mean bias ranges from -0.87%, which corresponds to -21.2 mm in ZTD (at EVPA, Ukraine, at
309 a distance of 96.5 km from the RS WMO 33946 station) to 0.68%, which corresponds to 15.4 mm
310 (at OBER, Germany at 90.8 km from RS WMO 11120). The overall mean ZTD bias for all sites is -
311 0.6 mm with a standard deviation of 4.9 mm. For more than 75% of the stations (178 pairs), the
312 agreement is below 5 mm in ZTD and only 5.5% of the stations (13 pairs) have ZTD biases higher
313 than 10 mm. The higher biases arise mostly for paired sites over 50 km away from each other, for
314 which differences in the geographical representativeness become important. For example, the GPS
315 stations OBER, OBE2 and OBET located in Oberpfaffenhofen (Germany) are collocated with the
316 RS WMO 11120 at Innsbruck Airport in Austria, on the opposite side of the North Chain in the
317 Karwendel Alps. Our results are in accordance with Wang et al. (2007), in which the authors
318 compared PW (not ZTD) from GPS and global radiosondes and reported an overall dry bias about
319 1.08 mm for the radiosondes. However, it should be noted that these obtained biases, in both our
320 and their study, are obtained from a mixture of radiosonde types, and daytime and nighttime
321 launches. For instance, in agreement with Wang et al. (2007), we also found a small negative (dry)
322 bias -1.19 mm for Vaisala radiosondes (our bias is inversely calculated), which is the most common
323 type used in Europe (81% of all used in this study). In this context, we mention that different
324 Vaisala radiosonde types (e.g. RS80 vs RS90/RS92) are equipped with different humidity sensors,
325 resulting in e.g. different RS-GPS comparisons in PW, both for nighttime and daytime comparisons
326 (e.g. Van Malderen et al., 2014). In addition, it must be remembered, that Wang et al. (2007) used
327 global radiosonde data from 2003 and 2004, while we used all available data over Europe from
328 1994 to 2015. For MRZ, GRAW and M2K2 (from MODEM) radiosonde types, which represent
329 4.6%, 3.4% and 3.0% of the compared radiosondes types respectively, we received a systematic
330 positive bias for the radiosondes, which can be interpreted as a moist bias, which is again in line
331 with the results of Wang et al. (2007) for these radiosonde types. On the other hand, the results for
332 M2K2 are at odds with Bock et al. (2013), in which a dry radiosonde bias in IWV compared to GPS

Formattato: Tipo di carattere: (asiatico) Times New Roman, Colore carattere: Nero, Inglese (Regno Unito)

Formattato: Tipo di carattere: (asiatico) Times New Roman, Non Corsivo, Colore carattere: Nero, Inglese (Regno Unito), Controllo ortografia e grammatica

Commentato [g22]: This is the radiosonde type: Vaisala RS90.

Commentato [g23]: M2K2 is a radiosonde type that Olivier Bock has assessed in his AMT paper (doi:10.5194/amt-6-2777-2013). Please comment if in this paper also a positive bias has been found.

Commentato [AA24]: Bock et al. (2013) report the dry bias for M2K2 radiosonde type. With respect to their results, our positive bias should be considered as moist bias and is not consistent with them. However, Bock et al. also noted that their results are not consistent with the nearby station in France.

was found at a French site. However, they also indicated that their results are not consistent with another nearby radiosonde station and needs further investigation. Further investigation in our study is also needed for several near or moved GPS stations, or switched radiosonde type at one station. For example in Brussels (Belgium) BRUS station, included in the EPN network since 1996, was replaced by BRUX in 2012. Their bias w.r.t. radiosonde (WMO code 6447) has opposite sign (-1.2 mm and 3.4 mm respectively). However, the radiosonde type was switched from RS80 to RS90 in 2007 (Van Malderen et al., 2014), which makes the bias for BRUS additionally affected by the change of the radiosonde type.

In agreement with Ning et al. (2012), the ZTD standard deviation generally increases with the distance from the radiosonde launch site. It is in the range of [0.16; 0.76] %, which corresponds to [3; 18] mm in ZTD, till 15 km (first band in Figure 10); in [0.29; 0.78] %, corresponding to [7; 19] mm, till 70 km (second band in Figure 10), and in [10; 33] mm till 133 km (third band in Figure 10). The numbers of the standard deviation are comparable with previous studies. Haase et al. (2001) showed a very good agreement with biases less than 5 mm in ZTD and a standard deviation of 12 mm for most of the analysed sites in Mediterranean. Similar results ($6.0 \text{ mm} \pm 11.7 \text{ mm}$) were obtained also by Vedel et al. (2001). Both studies were based on non-located pairs at sites less than 50 km from each other. Pacione et al (2011), considering 1-year of GPS ZTD and radiosonde data over the E-GVAP super sites network, obtained a standard deviation of 5-14 mm. Dousa et al. 2012 evaluated ZTDs from GNSS and radiosondes on a global scale over a 10-month period and reported a standard deviation of 5–16 mm.

If we compare both the EPN-Repro1 ZTD product (completed with the EUREF operational product after 30 December 2006) and the EPN-Repro2 with the radiosonde ZTDs for the same period 1996-2014, we found an improvement of approximately 3-4% in the overall standard deviation for the second processing.

4.2 Evaluation versus ERA-Interim data

We also compared the EPN-Repro2 ZTDs with the ZTDs calculated from ERA-Interim (Dee et al., 2011) from the European Centre for Medium-Range Weather Forecasts (ECMWF). The ERA-Interim is a re-analysis product of a Numerical Weather Prediction (NWP) model and is available every 6 hours (00, 06, 12, 18 UTC) with a horizontal resolution of 1×1 degree and with 60 vertical model levels.

For the period 1996-2014 and for each EPN station, the ZTD and tropospheric linear horizontal gradients were computed using the GFZ (German Research Centre for Geosciences) ray-tracing software (Zus et al., 2014). Combined EUREF Repro1 and Repro2 products as well as individual

Commentato [g25]: VRS80L is the radiosonde type: Vaisala RS80.

Commentato [g26]: In our AMT2014 paper, section 4.2, we also make the RS-GPS comparison separately for the two (or 3) radiosonde types that have been used at Brussels. As a matter of fact, we switched from RS80 to RS90 in August 2007. You are hence comparing BRUS with RS80 and RS90/RS92, while comparing BRUX only with RS92. This will have a non-negligible effect on the comparison, and is hence not related only to the change of the GPS station!

Commentato [AA27R26]: Included in the text.

ACs tropospheric parameters were assessed with the corresponding parameters estimated from the ERA-Interim re-analysis. The evaluation of GNSS and ERA-Interim was performed using the GOP-TropDB (Gyori and Dousa, 2016) by calculating parameter (ZTD, horizontal gradients, see below) differences for each station, using the values at every 6 hours (00:00, 06:00, 12:00 and 18:00), as available from the ERA-Interim model output. A linear temporal interpolation to those four timestamps was thus necessarily applied for all GNSS products, which are available in HH:30 timestamps as required for the combination process. As all compared GNSS products have the same time resolution (1 hour), the interpolation is assumed to affect all products in the same way. Therefore, we assume that all inter-comparisons to a common reference (ERA-Interim) principally reflect the quality of the products. No vertical corrections were applied since ERA-Interim variables were estimated for the long-term antenna reference position of each station.

Table 4 summarizes the mean total statistics of individual (ACs) and combined (EUREF) tropospheric parameters, ZTDs and horizontal gradients, over all available stations. The EUREF combined solution does not provide tropospheric gradients and these could therefore be evaluated for individual solutions only. In Table 4, a common ZTD bias (GNSS minus ERA-Interim) of about -1.8 mm is found for all GNSS solutions compared to ERA-Interim, but a large station to station variability could be noted, as is obvious from the estimated uncertainties. ZTD standard deviations are generally at the level of 8 mm between GNSS and ERA-Interim ZTDs, but with the IG0 solution performing about 25% worse than the others as already detected during the combination. Two solutions, AS0 and LP1 are slightly better than GO4 and MU2: with a standard deviation of 7.7 mm, their accuracy is at the level of the EUREF combined solution. The better performance of the AS0 solution can be explained by applying a stochastic troposphere modelling using original (not double-difference) observations sensitive to the absolute tropospheric delays, so that the true dynamics in the troposphere is better taken into account. LP1 included roughly one third of the EPN stations, properly selected according to the station quality, hereby making it difficult to interpret this difference with respect to those solutions processing the full EPN.

The comparison of tropospheric linear horizontal gradients (East and North) from GNSS and ERA-Interim revealed a problem with the MU2 solution (see Table 4). This solution shows a high inconsistency over different stations, which is not visible in the total statistics, but mainly in the uncertainties, which are an order or magnitude higher compared to all other solutions. A geographical plot (not shown here) confirmed this site-specific systematic effect, both in positive and negative sense. The impact was however not observed in the MU2 ZTD results. Additionally, the GO4 solution performed slightly worse than the others. This was identified as a consequence of

Formattato: Tipo di carattere: Non Corsivo, Controllo ortografia e grammatica

Commentato [g28]: Please specify how the bias is calculated.

Formattato: Tipo di carattere: Non Corsivo, Controllo ortografia e grammatica

Commentato [j29R28]: YES, GNSS minus ERA-Interim

Commentato [g30]: What do you mean by "undifference"?

Commentato [j31R30]: Original (not double-difference)

estimating 6-hour gradients using a piece-wise linear function without any absolute or relative constraints. In such case, higher correlations with other parameters occurred and increased the uncertainties of the estimates. For this purpose, the GO6 solution (not shown) was derived, fully compliant with the GO4, but stacking tropospheric gradients into 24 hours piece-wise linear modelling. In comparison with the former GO4 solution (Dousa and Vaclavovic, 2016), the GO6 standard deviations dropped from 0.38 mm to 0.28 mm and from 0.40 mm to 0.29 mm for East and North gradients, respectively, which corresponds to the LP1 solution that applied the same settings. Additionally, Dousa and Vaclavovic (2016) found a strong impact of a low-elevation receiver tracking problem on the estimation of the horizontal gradients, which was particularly visible when comparing with ERA-Interim horizontal gradients. Looking for systematic behaviour in monthly mean differences in the gradients therefore seems to be a useful indicator for instrumentation-related issues and should be applied as one of the tools for cleaning the EPN historical archive.

For completeness, we also evaluated the EPN-Repro1 ZTD product with respect to ERA-Interim using the same period, i.e. 1996-2014 (after completing again with the EUREF operational product, see above). Comparing EPN-Repro1 and EPN-Repro2 with the numerical weather model re-analysis showed a 8-9% improvement of EPN-Repro2 in both overall standard deviation and bias.

~~Figure 11~~ ~~Figure 11~~ shows the distributions of station mean biases and standard deviations of EPN-Repro1 and EPN-Repro2 ZTDs compared to ERA-Interim ZTDs using the whole period 1996-2014. Common reductions of both statistical characteristics are clearly visible for the majority of all stations. From the data of ~~Figure 11~~ ~~Figure 11~~, we also illustrate the site-by-site improvements in terms of ZTD bias, standard deviation and RMS in ~~Figure 12~~ ~~Figure 12~~. The calculated median improvements for these statistics reached 21.1 %, 6.8 % and 8.0 %, respectively, which corresponds to the abovementioned improvement of 8-9 %. A degradation of the standard deviation was found at three stations: SKE8 (Skellefteå, Sweden, integrated in the EPN since 28-09-2014), GARI (Porto Garibaldi, Italy, integrated in the EPN since 08-11-2009) and SNEC (Snezka, Czech Republic, former EPN station since 14-06-2009). These three stations provide much less data compared to other stations, 1%, 30% and 3%, respectively, of data pairs of other stations. All other stations (290) showed improvements. We found 72 stations with increased absolute bias in EPN-Repro2 compared to Repro1 while the other 221 stations (75%) had a reduced bias with ERA-Interim ZTD.

Time series of monthly mean biases and standard deviations for ZTD differences of EPN-Repro2 and ERA-Interim are shown in ~~Figure 13~~ ~~Figure 13~~. The small negative bias slowly decreases towards 2014, but the high uncertainty of the mean bias indicates a site-specific behaviour, depending mainly on latitude and altitude of the EPN station and the quality of both ERA-Interim

Formattato: Tipo di carattere: Non Corsivo

Formattato: Tipo di carattere: Non Corsivo

Formattato: Tipo di carattere: Non Corsivo

Commentato [g32]: I guess the order of Repro2 and Repro 1 should be changed in this sentence (otherwise EPN-Repro1 would be closer to ERA-interim than EPN-Repro2). Please check!!!

Commentato [j33R32]: YES, thank you.

Formattato: Tipo di carattere: Non Corsivo

432 and GNSS products. There is almost no seasonal signal observed in the time series of ZTD mean
433 biases or uncertainties, but clearly in the ZTD mean standard deviation and the uncertainties. The
434 increase of standard deviation in summer is due to more humidity in troposphere which is more
435 difficult to model accurately in both GNSS and ERA-interim. The slightly increasing standard
436 deviation towards 2014 can be attributed to the increase of number of stations in EPN: starting from
437 about 30 in 1996 and with more than 250 in 2014. A higher number of stations reduces the
438 variability in monthly mean biases, however, site-specific errors then contribute more to higher
439 values of standard deviation.

440 ~~Figure 14~~Figure 14 displays the geographical distribution of total ZTD biases and standard
441 deviations for all sites. Prevailing negative biases seem to become lower or even positive in the
442 mountain areas. There is no latitudinal dependence observed for ZTD biases in Europe, but a strong
443 one for standard deviations. This corresponds mainly to the increase of water vapour content and its
444 variability towards the equator.

445 4.3 Evaluation of ZTD trends

446 To illustrate the impact of the new processing on the resulting ZTD trends and related uncertainties,
447 we considered five EPN stations, among those with the longest time span: GOPE (Ondrejov, Czech
448 Republic, integrated in the EPN since 31-12-1995), METS (Kirkkonummi, Finland, integrated in
449 the EPN since 31-12-1995), ONSA (Onsala, Sweden, integrated in the EPN since 31-12-1995),
450 PENC (Penc, Hungary, integrated in the EPN since 03-03-2096) and WTZR (Bad Koetzing,
451 Germany, integrated in the EPN since 31-12-1995). For these five stations, we have computed ZTD
452 trends using EPN-Repro2, EPN-Repro1 (again completed with the EUREF operational products),
453 radiosonde and ERA-Interim data. Furthermore, those five stations also belong to the IGS Network,
454 for which IGS Repro1, completed with the IGS operational products, are available and extracted
455 from the GOP-TropDB, so that we could also calculate ZTD trends from this dataset.

456 First, we removed the annual signal from the original time series and marked all outliers according
457 to the 3-sigma criterion. Then, we tried to remove all inhomogeneities in the GPS ZTD time series,
458 related to instrumental changes, which might introduce a change in the mean of the ZTD time series
459 and therefore have an impact on the ZTD trends. In particular, for all GPS ZTD data sets we have
460 estimated all documented shifts in the mean related to the antenna replacement. No other
461 unexplained break points has been corrected for, to be sure not to introduce any artificial errors.
462 Based on these cleaned and filtered data, we have used, independently, a linear regression model
463 before and after the considered epoch of the offset. The difference of the mean ZTDs between those
464 two linear regression models is then considered as the offset of the specific epoch is. With this

Commentato [g34]: Explain shortly where this seasonality comes from.

Commentato [j35R34]: explained

Formattato: Tipo di carattere: Non Corsivo

465 technique, we removed all the estimated offsets from the original GPS ZTD time series. Generally,
466 the amplitudes of the offsets are much lower than the noise level and depend on the applied method
467 of estimation. Therefore, the final ZTD trends and uncertainties presented here are affected by the
468 used methodology and should not be considered in absolute terms. No homogenization has been
469 done for the radiosonde data, since reliable metadata are not available. Also the ERA-Interim ZTD
470 time series were not corrected for inhomogeneities. Finally, a Least Squares Estimation method has
471 been applied to estimate the linear trends and the seasonal components.

472 In ~~Figure 15~~Figure 15, the ZTD trends and uncertainties are presented for the five sites and for all
473 ZTD datasets. First of all, it should be noted that the trends between the three GPS ZTD data sets
474 are very consistent (as long as the same homogenisation procedure is applied). The overall RMS
475 among trends estimated from GPS measurements is 0.02 mm/year. If we now consider all five ZTD
476 sources, the best agreement between the ZTD trends is achieved at ONSA (RMS = 0.04 mm/year)
477 and WTZR (RMS = 0.02 mm/year). For PENC, we also have a good agreement of the GPS ZTD
478 trends with respect to ERA-Interim (RMS = 0.05 mm/year), but a large discrepancy with the
479 radiosonde ZTD trend is found (RMS = -0.31 mm/year). This large discrepancy is probably due to
480 the distance to the radiosonde launch site (40.7 km, RS WMO 12843) and to the lack of
481 homogenization of the radiosonde data. For the five considered stations, the agreement of GPS ZTD
482 trends with respect to ERA-Interim (RMS = 0.11 mm/year) is better than with respect to
483 radiosondes (RMS = 0.16 mm/year). Even although, for the five considered stations, EPN-Repro2
484 do not change significantly the value of the ZTD trends with respect to EPN-Repro1, it has a less
485 uncertainty (the improvement is 6.9%) of ZTD trends, better agreement with ERA-Interim (the
486 improvement is 8.0%) ZTD trends and a slightly worse agreement with the radiosonde (the
487 degradation is 3.8%). However, one should keep in mind that time series from radiosonde
488 measurements were not homogenized and their trends may not be necessarily trustworthy. Over
489 Europe, the EPN network has a better spatial resolution than the IGS and radiosonde networks,
490 which are used today for an observations-based long-term analysis of ZTD/IWV variability. Taking
491 into account the good consistency among the ZTD trends, EPN-Repro2 can be used for trend
492 detection in areas where other data are not available.

493 5. Conclusions

494 In this paper, we described the activities carried out in the framework of the EPN second
495 reprocessing campaign. We focused on the tropospheric products homogeneously reprocessed by
496 five EPN Analysis Centres for the period 1996-2014 and we described the ZTD combined product.
497 We evaluated the impact of few diversities among the provided GNSS solutions. The inclusion of

Formattato: Tipo di carattere: Non Corsivo, Controllo ortografia e grammatica

Commentato [g36]: Overall RMS between the 3 GPS ZTD trends?

Commentato [AA37R36]: Yes.

Commentato [g38]: Add a number here to proof this statement.

Commentato [AA39R38]: Done.

Commentato [g40]: I think this analysis deserves a separate section and does not belong to the conclusions. In the conclusion, you should just give a wrap up, and not describing new research. I also seriously changed the text. Please go through it and check thoroughly if you could live with every modification I propose!

Commentato [AA41R40]: It is ok!

498 additional GLONASS observations in the GNSS processing has a neutral impact on the ZTD trend
499 analysis pointing out that the ZTD trends might be determined independently of the satellite
500 systems used in the processing (see Section 2.1). The inconsistencies in the ZTD time series due to
501 different antenna calibration models (see Section 2.2) are not large enough to be captured during the
502 combination process (see Section 3), where a 10 mm threshold in the ZTD bias (about 1.5 kg/m²
503 IWV) is set in order to flag problematic ACs or stations. The effect on the ZTDs of non-tidal
504 atmospheric loading correction (see Section 2.3) seems to be negligible. We assessed the quality of
505 the ZTD combined product, which is below 3 mm before GPS week 1055 and 2 mm thereafter. This
506 is related to the worse quality of data and products during the first years of the EPN/IGS activities.

507 Both individual and combined tropospheric products, along with reference coordinates and other
508 metadata, are stored in a SINEX TRO format (Gendt, G. 1997), and are available to the users at the
509 EPN Regional Data Centres (RDC), located at BKG (Federal Agency for Cartography and Geodesy,
510 Germany). For each EPN station, plots on ZTD time series, ZTD monthly means, comparison with
511 radiosonde data (if collocated), and comparison versus the ERA-Interim data will be available at the
512 EPN Central Bureau (Royal Observatory of Belgium, Brussels, Belgium).

513 We showed in section 4.1 that EPN-Repro2 led to an improvement of approximately 3-4% in the
514 overall standard deviation in the ZTD differences with radiosonde data, as compared with EPN-
515 Repro1.

516 The assessment of the EPN-Repro2 comparison with the ERA-Interim re-analysis showed a 8-9%
517 improvement in both the overall ZTD bias and standard deviation with respect to EPN-Repro1 for
518 the majority of the stations (see Section 4.2). Comparisons of the GNSS solutions with ERA-
519 Interim, showed the agreement in ZTD at the level of 8-9 mm, however, site-specific performance
520 ranging from 5 mm to 15 mm for standard deviations and from -7 mm to 3 mm for biases
521 considering 99% of results roughly.

522 The use of ground-based GNSS long-term data for climate research is an emerging field. For
523 example, for the assessment of Euro-CORDEX (Coordinated Regional Climate Downscaling
524 Experiment) climate model simulation, the IGS Repro1dataset (Byun and Bar-Sever, 2009) has
525 been used as reference reprocessed GPS products (Bastin et al. 2016). However, this dataset is quite
526 sparse over Europe (only 85 stations over the 280 EPN stations) and covers only the period 1996-
527 2010. As pointed by Baldysz et al. (2015, 2016) an additional two years of ZTD data can change the
528 estimated trends up to 10%. Therefore, with data after 2010 and with a better coverage over Europe,
529 EPN-Repro2 can be used as a reference data set with a high potential for monitoring the trends and
530 variability in atmospheric water vapour as reported in Section 4.3. As a matter of fact, a comparison

Commentato [RVM42]: For which parameter?

Commentato [PR43R42]: yes

Commentato [g44]: I think you should investigate some more time on the summary of the most important findings of this paper. Do not forget that a lot of readers start by reading the abstract and the conclusions and then make up their mind if they proceed with the rest. In its current form, this summary is not very attracting. Do not forget to mention the most important findings of sections 2 and 3 (e.g. one sentence for every subsection of 2).

531 between GNSS IWV, computed from EPN-Repro2 ZTD data for SOFI (Sofia, Bulgaria) by the
532 Sofia University, and ALADIN-Climate IWV simulations conducted by the Hungarian
533 Meteorological Service, is performed for the period 2003-2008 at the moment. The preliminary
534 results show a tendency of the model to underestimate IWV. Clearly, a larger number of model grid
535 points need to be investigated in different regions in Europe and the EPN-Repro2 data is well suited
536 for this.

537 The reprocessing activity of the five EPN ACs was a huge effort generating homogeneous products
538 not only for station coordinates and velocities, but also for tropospheric products. The knowledge
539 gained will certainly help for a next reprocessing activity. A next reprocessing will most likely
540 include Galileo and BeiDou data and therefore it will be started in some years from now after
541 having successfully integrated these new data in the current operational near real-time and daily
542 products of EUREF. The consistent use of identical models in various software packages is another
543 challenge for the future and would enable to improve the consistency of the combined solution.
544 Prior to any next reprocessing, it was agreed in EUREF to focus on cleaning and documenting the
545 data in the EPN historical archive as it should highly facilitate any future work. For this purpose, all
546 existing information needs to be collected from all the levels of data processing, combination and
547 evaluation, which includes initial GNSS data quality checking, generation of individual daily
548 solutions, combination of individual coordinates and ZTDs, long-term combination for velocity
549 estimates and assessments of ZTDs and gradients with independent data sources.

550

551 *Author Contributions.* R. Pacione coordinated the writing of the manuscript and wrote section 1, 2,
552 3 and 4.1. A. Araszkiewicz wrote section 2.2 and 2.3, 4.3 and contributed to section 4.1. E.
553 Brockmann wrote section 2.1. J. Dousa wrote section 4.2. All authors contributed to section 5. All
554 authors approved the final manuscript before its submission.

555

556 **Acknowledgments**

557 The authors would like to acknowledge the support provided by COST – (European Cooperation in
558 Science and Technology) for providing financial assistance for the publication of the paper. The
559 authors thank the members of the EUREF project “EPN reprocessing”. e-GEOS work is done
560 under ASI Contract 2015-050-R.0. The assessments of the EUREF combined and individual
561 solutions in the GOP-TropDB were supported by the Ministry of Education, Youth and Science,
562 the Czech Republic (project LH14089). The MUT AC contribution was supported by statutory
563 funds at the Institute of Geodesy, Faculty of Civil Engineering and Geodesy, Military

564 University of Technology (No. PBS/23-933/2016). Finally, we thank the two anonymous
565 referees and the Associate Editor Dr. Roeland Van Malderen for their comments which helped
566 much to improve the paper.

567
568 **References**

569 Alshawaf, F., Balidakis, K., Dick, G., Heise, S., and Wickert, J.: Estimating trends in atmospheric
570 water vapor and temperature time series over Germany, *Atmos. Meas. Tech. Discuss.*, in discussion,
571 2017.

572 Araszkiewicz, A., and Voelksen, C.: The impact of the antenna phase center models on the
573 coordinates in the EUREF Permanent Network, *GPS Solut.*, doi: 10.1007/s10291-016-0564-7, 2016.

574 Baldysz, Z., Nykiel, G., Figurski, M., Szafranek, K., and Kroszczynski, K.: Investigation of the 16-
575 year and 18-year ZTD Time Series Derived from GPS Data Processing. *Acta Geophys.* 63, 1103-
576 1125, DOI: 10.1515/acgeo-2015-0033, 2015.

577 Baldysz Z., Nykiel G., Araszkiewicz A., Figurski M. and Szafranek K.: Comparison of GPS
578 tropospheric delays derived from two consecutive EPN reprocessing campaigns from the point of
579 view of climate monitoring. *Atmos. Meas. Tech.*, 9, 4861-4877, DOI: 10.5194/amt-9-4861-2016,
580 2016.

581 Bastin, S., Bock, O., Chiriaco, M., Conte, D., Dominguez, M., Roehring, R., Drobinski, P.,
582 Parracho, A.: Evaluation of MED-CORDEX simulations water cycle at different time scale using
583 long-term GPS-retrieved IWV over Europe, presentation at COST ES1206 workshop, Potsdam
584 (Germany) 1-2 September 2016.

585 Bevis, M., Businger, S., Herring, T. A., Rocken C., Anthes, R. A., and Ware, R. H.: GPS
586 Meteorology: Remote Sensing of 20 Atmospheric Water Vapour Using the Global Positioning
587 System, *J. Geophys. Res.*, 97, 15787–15801, 1992.

588 Bevis M., S. Businger, S. Chiswell, T. A. Herring, R. A. Anthes, C. Rocken, and Ware, R. H.: GPS
589 Meteorology: Mapping Zenith Wet Delays onto Precipitable Water. *J. Appl. Meteorol.*, 33, 379-386,
590 1994.

591 Byun S. H., and Bar-Sever, Y. E.: A new type of troposphere zenith path delay product of the
592 International GNSS Service. *J. Geod.*, 83(3-4), 1–7, 2009.

593 Bock, O., Bosser, P., Bourcy, T., David, L., Goutail, F., Hoareau, C., Keckhut, P., Legain, D.,
594 Pazmino, A., Pelon, J., Pipis, K., Poujol, G., Sarkissian, A., Thom, C., Tournois, G., and Tzanos, D.:
595 Accuracy assessment of water vapour measurements from in situ and remote sensing techniques
596 during the DEMEVAP 2011 campaign at OHP, *Atmos. Meas. Tech.*, 6, 2777-2802,
597 doi:10.5194/amt-6-2777-2013, 2013.

598 Bock, O., P. Bosser, R. Pacione, M., Nuret, N. Fourrie, and Parracho, A.: A high quality
599 reprocessed ground-based GPS dataset for atmospheric process studies, radiosonde and model
600 evaluation, and reanalysis of HYMEX Special Observing Period, *Q. J. Roy. Meteor. Soc.*, doi:
601 10.1002/qj.2701, 2015.

602 Boehm, J., and Schuh, H.: Vienna mapping functions in VLBI analyses, *Geophys. Res. Lett.*, 31,
603 L01603, doi: 10.1029/2003GL018984, 2004.

Commentato [RVM45]: Please check if the format and journal abbreviations are compliant with AMT's recommendations

604 Boehm, J., A. Niell, P. Tregoning, and Schuh, H.: Global Mapping Function (GMF): A new
605 empirical mapping function based on numerical weather model data, *Geophys. Res. Lett.*, 33,
606 L07304, doi: 10.1029/2005GL025546, 2006a.

607 Boehm, J., B. Werl, and Schuh, H.: Troposphere mapping functions for GPS and very long baseline
608 interferometry from European Centre for Medium-Range Weather Forecasts operational analysis
609 data, *J. Geophys. Res.*, 111, B02406, doi: 10.1029/2005JB003629, 2006b.

610 Bruyninx, C., Habrich, H., Söhne, W., Kenyeres, A., Stangl, G., Völksen, C.: Enhancement of the
611 EUREF Permanent Network Services and Products, *Geodesy for Planet Earth*, IAG Symposia
612 Series, 136: 27–35. doi: 10.1007/978-3-642-20338

613 Bruyninx, C., Araszkiewicz, A., Brockmann, E., Kenyeres, A., Pacione, R., Söhne, W., Stangl, G.,
614 Szafrank K., and Völksen, C.: EPN Regional Network Associate Analysis Center Technical Report
615 2015, IGS Technical Report 2015, Editors Yoomin Jean and Rolf Dach, Astronomical Institute,
616 University of Bern, 2015, pp. 101-110, 2015.

617 COST-716 Exploitation of Ground-Based GPS for Operational Numerical Weather Prediction and
618 Climate Applications – Final Report, in: Elgered, G., Plag, H.-P., Van der Marel, H., et al. (Eds.),
619 EUR 21639, 2005.

620 Dach, R., Hugentobler, U., Fridez, P., and Meindl, M.: Bernese GPS Software Version 5.0, *J.*
621 *Geophys. R.-Atmos.*, 119, doi: 10.1002/2013JD021124, 2014.

622 Dach, R., J. Böhm, S. Lutz, P. Steigenberger and Beutler, G.: Evaluation of the impact of
623 atmospheric pressure loading modeling on GNSS data analysis, *J. Geodesy* doi: 10.1007/s00190-
624 010-0417-z, 2010.

625 Dee, D. P., Uppala, S. M., Simmons, A. J., Berrisford, P., Poli, P., Kobayashi, S., Andrae, U.,
626 Balmaseda, M. A., Balsamo, G., Bauer, P., Bechtold, P., and Beljaars, A. C. M.: The ERA-Interim
627 reanalysis: Configuration and performance of the data assimilation system, *Q. J. Roy. Meteor. Soc.*,
628 137(656), 553–597, 2011.

629 Desai, S. D., W. Bertiger, M. Garcia-Fernandez, B. Haines, N. Harvey, C. Selle, A. Sibthorpe, A.
630 Sibois, and Weiss, J. P.: JPL's Reanalysis of Historical GPS Data from the Second IGS Reanalysis
631 Campaign, AGU Fall Meeting, San Francisco, CA, 2014.

632 Dow, J.M., Neilan, R. E., and Rizos, C.: The International GNSS Service in a changing landscape
633 of Global Navigation Satellite Systems, *J. Geodesy* 83:191–198, doi: 10.1007/s00190-008-0300-3,
634 2009.

635 Dousa, J. and G.V. Bennett: Estimation and Evaluation of Hourly Updated Global GPS Zenith
636 Total Delays over ten Months, *GPS Solut.*, 17(4):453–464, doi:10.1007/s10291-012-0291-7, 2012.

637 Dousa, J. and Vlacavovic, P.: Tropospheric products of the 2nd European reprocessing (1996–2014),
638 *Atmos. Meas. Tech. Discuss.*, doi:10.5194/amt-2017-11, in review, 2017.

639 Gendt, G. SINEX TRO—Solution (Software/technique) INdependent Exchange Format for
640 combination of TROpospheric estimates Version 0.01, March 1,
641 1997:https://igscb.jpl.nasa.gov/igscb/data/format/sinex_tropo.txt, 1997.

Commentato [RVM46]: Please use consistent journal abbreviations. You can find a list of the advised abbreviations on the journal web page.

Commentato [AA47R46]: Done!

Commentato [RVM48]: Same remark as here above.

Gyori, G., and Douša, J.: GOP-TropDB developments for tropospheric product evaluation and monitoring – design, functionality and initial results, In: IAG Symposia Series, Rizos Ch. and Willis P. (eds), Springer Vol. 143, pp. 595-602., 2016

Guerova, G., Jones, J., Douša, J., Dick, G., de Haan, S., Pottiaux, E., Bock, O., Pacione, R., Elgered, G., Vedel, H., and Bender, M.: Review of the state of the art and future prospects of the ground-based GNSS meteorology in Europe, *Atmos. Meas. Tech.*, 9, 5385-5406, doi:10.5194/amt-9-5385-2016, 2016. IERS Conventions (2010). Gérard Petit and Brian Luzum (eds.). (IERS Technical Note ; 36) Frankfurt am Main: Verlag des Bundesamts für Kartographie und Geodäsie, 2010. 179 pp., ISBN 3-89888-989-6, 2010.

Ihde, J., Habrich, H., Sacher, M., Söhne, W., Altamimi, Z., Brockmann, E., Bruyninx, C., Caporali, C., Dousa, J., Fernandes, R., Hornik, H., Kenyeres, A., Lidberg, M., Mäkinen, J., Poutanen, M., Stangl, G., Torres, J.A., Völksen, C., (2013). EUREF's contribution to national, European and global geodetic infrastructures. IAG Symposia, vol. 139, pp. 189–196. doi: 10.1007/978-3-642-37222-3_24.

Jin, S.G., Park, J., Cho, J., and Park, P.: Seasonal variability of GPS-derived Zenith Tropospheric Delay (1994-2006) and climate implications, *J. Geophys. Res.*, 112, D09110, doi: 10.1029/2006JD007772, 2007.

Haase, J., Calais, E., Talaya, J., Rius, A., Vespe, F., Santangelo, R., Huang, X.-Y., Davila, J. M., Ge, M., Cucurull, L., Flores, A., Sciarretta, C., Pacione, R., Bocculari, M., Pugnaghi, S., Vedel, H., Mogensen, K., Yang, X., and Garate, J.: The contributions of the MAGIC project to the COST 716 objectives of assessing the operational potential of ground-based GPS meteorology on an international scale, *Physics and Chemistry of the Earth, Part A*, 26, 433–437, 2001.

Haase, J.S., H. Vedel, M. Ge, and E. Calais: GPS zenith tropospheric delay (ZTD) variability in the Mediterranean, *Phys. Chem. Earth (A)* 26(6–8):439–443, 2001.

Haase, J., M. Ge, H. Vedel, and Calais, E.: Accuracy and variability of GPS Tropospheric Delay Measurements of Water Vapor in the Western Mediterranean, *J. Appl. Meteorol.*, 42, 1547-1568, 2003.

King, R., Herring, T., and McClusky, S.: Documentation for the GAMIT GPS analysis software 10.4., Tech. rep., Massachusetts Institute of Technology, 2010.

Lutz, S., P. Steigenberger, G. Beutler, S. Schaer, R. Dach, and Jaggi, A.: GNSS orbits and ERPs from CODE's repro2 solutions, IGS Workshop Pasadena (USA), June 23–27, 2014.

Nilsson, T. and Elgered, G.: Long-term trends in the atmospheric water vapor content estimated from ground-based GPS data. *J. Geophys. Res.*, 113, doi: 10.1029/2008JD010110, 2008.

Ning, T., R. Haas, G. Elgered, and Willén U: Multi-technique comparisons of 10 years of wet delay estimates on the west coast of Sweden, *J. Geodesy* 86: 565. doi: 10.1007/s00190-011-0527-2, 2012.

Ning, T., J. Wickert, Z. Deng, S. Heise, G. Dick, S. Vey, and Schone, T.: Homogenized time series of the atmospheric water vapor content obtained from the GNSS reprocessed data, *J. Climate*, doi: 10.1175/JCLI-D-15-0158.1, 2016a

Ning, T., J. Wang, G. Elgered, G. Dick, J. Wickert, M. Bradke, M. Sommer, R. Querel, and Smale, D.: The uncertainty of the atmospheric integrated water vapour estimated from GNSS observations *Atmos. Meas. Tech.*, 9, 79-92, doi:10.5194/amt-9-79-2016, 2016b.

683 Mangiarotti, S., A. Cazenave, L. Soudarin and Crétau, J. F.: Annual vertical crustal motions
684 predicted from surface mass redistribution and observed by space geodesy, *J. Geophys. Res.*, 106,
685 B3, 4277, 2001.

686 Pacione, R., B. Pace, S.de Haan, H. Vedel, R.Lanotte, and Vespe, F.: Combination Methods of
687 Tropospheric Time Series, *Adv. Space Res.*, 47(2) 323-335 doi: 10.1016/j.asr.2010.07.021, 2011.

688 Petrov, L. and Boy, J.-P.: Study of the atmospheric pressure loading signal in very long baseline
689 interferometry observations," *J. Geophys. Res.*, 109, B03405, 14 pp., doi: 10.1029/2003JB002500,
690 2004.

691 Ray, R. D. and Ponte, R. M.: Barometric tides from ECMWF operational analyses, *Ann. Geophys.*,
692 21(8), pp. 1897-1910, doi: 10.5194/angeo-21-1897-2003.

693 Saastamoinen, J.: Contributions to the theory of atmospheric refraction, *Bull. Geodes.*, 107, 13–34,
694 doi:10.1007/BF02521844, 1973.

695 Santerre R.: Impact of GPS Satellite sky distribution. *Manuscr. Geod.*, 16, 28-53, 1991.

696 Schmid, R., Dach, R., Collilieux, X., Jäggi, A., Schmitz, M., Dilssner, F.: Absolute IGS antenna
697 phase center model igs08.atx: status and potential improvements, *J. Geodesy* 90(4):343–364,
698 doi:10.1007/s00190-015-0876-3

699 Sohn, D.-H., and Cho, J.: Trend Analysis of GPS Precipitable Water Vapor Above South Korea
700 Over the Last 10 Years, *J. Astron. Space Sci.* 27(3), 231-238 , doi: 10.5140/JASS.2010.27.3.231,
701 2010.

702 Suparta, W.: Validation of GPS PWV over UKM Bangi Malaysia for climate studies, *Procedia*
703 *Engineering* 50, 325 – 332, 2012.

704 Steigenberger, P., Tesmer, V., Krugel, M., Thaller, D., Schmid, R., Vey, S., and Rothacher, M.:
705 Comparisons of homogeneously reprocessed GPS and VLBI long time-series of troposphere zenith
706 delays and gradients, *J. Geod.*, 81(6-8), 503–514, doi: 10.1007/s00190-006-0124-y, 2007.

707 Tesmer, V., J. Boehm, R. Heinkelmann and Schuh, H.: Effect of different tropospheric mapping
708 functions on the TRF, CRF and position time-series estimated from VLBI, *J. Geodesy* 81, 409-421,
709 doi:10.1007/s00190-006-0126-9, 2007.

710 Tregoning, P., and T. van Dam: Atmospheric pressure loading corrections applied to GPS data at
711 the observation level, *Geophys. Res. Lett.*, 32, L22310, doi:10.1029/2005GL024104, 2005

712 Tregoning P., Watson C.: Atmospheric effects and spurious signals in GPS analyses. *J. Geophys.*
713 *Res.*, 114, B09403, doi: 10.1029/2009JB006344, 2009.

714 Van Dam, T., G. Blewitt, and Heflin, M. B.: Atmospheric pressure loading effects on Global
715 Positioning System coordinate determinations, *J. Geophys. Res.*, 99, B12, 23939, 1994.

716 Van Malderen, R., Brenot, H., Pottiaux, E., Beirle, S., Hermans, C., De Mazière, M., Wagner, T.,
717 De Backer, H., and Bruyninx, C.: A multi-site intercomparison of integrated water vapour
718 observations for climate change analysis, *Atmos. Meas. Tech.*, 7, 2487-2512, doi:10.5194/amt-7-
719 2487-2014, 2014.

720 Vey, S., R. Dietrich, M. Fritsche, A. Rulke, P. Steigenberger, and Rothacher, M.: On the
721 homogeneity and interpretation of precipitable water time series derived from global GPS
722 observations, *J. Geophys. Res.*, 114, D10101, doi: 10.1029/2008JD010415, 2009.

Commentato [RVM49]: For Nilsson and Elgered, you are using *J. Geophys. Res.* as journal abbreviation. Be consistent, also with the advised list of journal abbreviations.

723 Voelksen, C.: An update on the EPN Reprocessing Project: Current Achievements and Status,
 724 Presented at EUREF 2011 Symposium, Chisinau, Republic of Moldova, May 25-28 2011,
 725 [http://www.epncb.oma.be/_documentation/papers/eurefsymposium2011/an_update_on_epn_reproc](http://www.epncb.oma.be/_documentation/papers/eurefsymposium2011/an_update_on_epn_reprocessing_project_current_achievement_and_status)
 726 [essing_project_current_achievement_and_status](http://www.epncb.oma.be/_documentation/papers/eurefsymposium2011/an_update_on_epn_reprocessing_project_current_achievement_and_status), 2011.

727 Wang, J., Zhang, L., Dai, A., Van Hove, T., Van Baelen, J.: A near-global, 2-hourly data set of
 728 atmospheric precipitable water dataset from ground-based GPS measurements, *J. Geophys. Res.*
 729 112(D11107). doi:10.1029/2006JD007529, 2007.

730 Wang, J. and Zhang, L.: Climate applications of a global, 2-hourly atmospheric precipitable water
 731 dataset derived from IGS tropospheric products, *J. Geodesy* 83: 209. doi: 10.1007/s00190-008-
 732 0238-5, 2009.

733 Webb, F. H., and Zumberge, J.F.: An Introduction to GIPSY/OASIS II. JPL D-11088, 1997.

734 Vedel, H., K. S. Mogensen, and X.-Y. Huang: Calculation of zenith delays from meteorological
 735 data comparison of NWP model, radiosonde and GPS delays, *Phys. Chem. Earth Pt. A*, 26, 497–
 736 502, doi: 10.1016/S1464-1895(01)00091-6, 2001.

737 Zus, F, Dick, G, Heise, S, Dousa, J, and Wickert J.: The rapid and precise computation of GPS slant
 738 total delays and mapping factors utilizing a numerical weather model, *Radio Sci.*, 49(3): 207-216,
 739 doi: 10.1002/2013RS005280, 2014.

740

741 **Table**

742 **Table Captions**

743 ~~Table 1: EPN Analysis Centres providing EPN-Repro2 solutions~~
744 ~~Table 1: EPN Analysis Centres providing EPN-Repro2 solutions.~~

745 ~~Table 2: EPN-Repro2 processing options for each contributing solutions. AS0 solution is provided~~
746 ~~by ASI/CGS (Matera, Italy), GO0, GO1 and GO4 solutions are provided by GOP (Pecny, Czech~~
747 ~~Republic), IG0 solution by IGE (Madrid, Spain), LP0 and LP1 solutions by LPT (Waben,~~
748 ~~Switzerland), and MU2 and MU4 solutions by MUT (Warsaw, Poland).~~
749 ~~Table 2: EPN-Repro2 processing options for each contributing solutions. AS0 solution is provided by ASI/CGS (Matera,~~
750 ~~Italy), GO0, GO1 and GO4 solutions are provided by GOP (Pecny, Czech Republic), IG0 solution~~
751 ~~by IGE (Madrid, Spain), LP0 and LP1 solutions by LPT (Waben, Switzerland), and MU2 and MU4~~
752 ~~solutions by MUT (Warsaw, Poland).~~

753 ~~Table 3. Percentage of red, orange and yellow biases (see text) for each contributing solution~~
754 ~~Table 3. Percentage of red, orange and yellow biases (see text) for each contributing solution.~~

755 ~~Table 4. Mean statistics and uncertainties, calculated from results of individual stations, provided~~
756 ~~for AC individuals and EUREF combined (Repro1 and Repro2) tropospheric parameters compared~~
757 ~~to the ERA-Interim re-analysis (EGRD = east gradient, NGRD = north gradient)~~
758 ~~Table 4. Mean statistics and uncertainties, calculated from results of individual stations, provided for AC~~
759 ~~individuals and EUREF combined (Repro1 and Repro2) tropospheric parameters compared to the~~
760 ~~ERA-Interim re-analysis (EGRD = east gradient, NGRD = north gradient)~~

Formattato: Inglese (Regno Unito)

Formattato: Tipo di carattere: Non Corsivo, Inglese (Regno Unito)

Formattato: Inglese (Regno Unito)

Formattato: Inglese (Regno Unito)

Formattato: Tipo di carattere: Non Corsivo, Controllo ortografia e grammatica

Formattato: Tipo di carattere: Non Corsivo, Controllo ortografia e grammatica

Formattato: Tipo di carattere: Non Corsivo

AC	Full name	City	Country	SW	EPN Network
ASI	Agenzia Spaziale Italiana	Matera	Italy	GIPSY-OASIS II	Full EPN
GOP	Geodetic Observatory	Pecny	Czech Republic	Bernese	Full EPN
IGE	National Geographic Institute	Madrid	Spain	Bernese	EPN-Subnetwork
LPT	Federal Office of Topography	Wabern	Switzerland	Bernese	EPN-Subnetwork
MUT	Military University of Technology	Warsaw	Poland	GAMIT	Full EPN

Table 1: EPN Analysis Centres providing EPN-Repro2 solutions.

	AS0	GO0	GO1	GO4	IG0	LP0	LP1	MU2	MU4
SOFTWARE	GIPSY 6.2	Bernese 5.2			Bernese 5.2	Bernese 5.2		GAMIT 10.5	
GNSS	GPS	GPS			GPS + GLONASS	GPS+GLONASS		GPS	
SOLUTION TYPE	PPP	Network			Network	Network		Network	
STATIONS	Full EPN	Full EPN			EPN Subnetwork	EPN Subnetwork		Full EPN	
ORBITS	JPL R2	CODE R2			CODE R2	CODE R2		CODE R2	
ANTENNAS	IGS08	IGS08 + Individual.			IGS08+ Individual.	IGS08	IGS08 + Individual.	IGS08 + Individual	IGS08
IERS	2010	2010			2010	2010		2010	
GRAVITY	EGM08	EGM08			EGM08	EGM08		EGM08	
TROPOSPHERE Estimated Parameters	ZTD (5min) GRAD (5min)	ZTD (1h) GRAD (6h)			ZTD (1h) GRAD (6h)	ZTD (1h) GRAD (24h)		ZTD (1h) GRAD (24h)	
MAPPING FUNCTION	VMF	GMF	VMF1	VMF	GMF	GMF	VMF	VMF	
ZTD/GRAD time stamp	hh:30 24 estimates/day	hh:30 (and hh:00) 24(+24) estimates/day			hh:30 24 estimates/day	hh:30 (and hh:00) 24(+24) estimates/day		hh:30 24 estimates/day	
IONOSPHERE	HOI included	CODE, HOI included			CODE (HOI included)	CODE (HOI included)		CODE IONEX + IGRF11 (HOI included)	
REFERENCE FRAME	IGb08	IGb08			IGb08	IGb08		IGb08	
OCEAN TIDES	FES2004	FES2004			FES2004	FES2004		FES2004	
TIDAL-ATMOSPHERIC LOADING	NO	NO			YES	YES	YES	YES	
NON-TIDAL-ATMOSPHERIC LOADING	NO	NO	NO	YES	NO	NO	YES	NO	
ELEVATION CUTOFF	3	3			3	3		5	
Delivered SNX_TRO Files [from week to week]	0834-1824	0836-1824			0835-1816	0835-1802		0835-1824	

Commentato [RVM50]: Precise Point Positioning, write out or use a footnote.

Commentato [PR51R50]: Done in the caption

Table 2: EPN-Repro2 processing options for each contributing solutions. AS0 solution is provided by ASI/CGS (Matera, Italy), GO0, GO1 and GO4 solutions are provided by GOP (Pecny, Czech Republic), IG0 solution by IGE (Madrid, Spain), LP0 and LP1 solutions by LPT (Waben, Switzerland), and MU2 and MU4 solutions by MUT (Warsaw, Poland). (PPP=Precise Point Positioning; GMF=Global Mapping Function; VMF=Vienna Mapping Function).

Solution	%Red bias	% Orange bias	% Yellow bias
AS0	17	27	56
G00	10	22	67
G01	12	23	65
G04	12	23	65
IG0	22	14	64
LP0	10	12	79
LP1	10	12	78
MU2	3	15	82

770 Table 3. Percentage of red, orange and yellow biases (see text) for each contributing solution.

771

Solution	ZTD bias [mm]	ZTD sdev [mm]	EGRD bias [mm]	EGRD sdev [mm]	NGRD bias [mm]	NGRD sdev [mm]
AS0 (full EPN)	-1.7±2.0	7.7±1.9	0.00±0.06	0.32±0.09	0.09±0.06	0.33±0.10
GO4 (full EPN)	-1.9±2.4	8.1±2.1	-0.04±0.09	0.38±0.10	0.00±0.09	0.40±0.12
MU2 (full EPN)	-1.8±2.0	8.3±2.1	-0.03±0.32	0.35±2.46	-0.01±0.84	0.34±2.37
IG0 (part EPN)	-1.6±2.3	10.7±2.2	-0.05±0.09	0.33±0.11	0.04±0.12	0.36±0.12
LP1 (part EPN)	-1.7±2.4	7.7±1.7	-0.02±0.06	0.28±0.05	0.03±0.09	0.27±0.06
EUR Repro2	-1.8±2.1	7.8±2.2	-	-	-	-
EUR Repro1	-2.2±2.3	8.5±2.1	-	-	-	-

Table 4. Mean statistics and uncertainties, calculated from results of individual stations, provided for AC individuals and EUREF combined (Repro1 and Repro2) tropospheric parameters compared to the ERA-Interim re-analysis (EGRD = east gradient, NGRD = north gradient)

776 **Figure**

777 **Figure Captions**

778 Figure 1. Time series of the number of GNSS observations for the period 1996-2014. GPS
779 observations are shown in red, GPS+GLONASS in blue and their differences in green. The
780 difference becomes significant starting from 2008.Figure 1. Time series of the number of GNSS
781 observations for the period 1996-2014. GPS observations are shown in red, GPS+GLONASS in
782 blue and their differences in green. The difference becomes significant starting from 2008.

783 Figure 2. ZTD trend differences between GPS only and GPS+GLONASS, computed over 111 sites.
784 The rate is in violet (primary y-axis) and the number of used differences is in green (secondary y-
785 axis).Figure 2. ZTD trend differences between GPS only and GPS+GLONASS, computed over 111
786 sites. The rate is in violet (primary y axis) and the number of used differences is in green
787 (secondary y-axis).

788 Figure 3. EPN station KLOP (Kloppenheim, Frankfurt, Germany) ZTD differences time series
789 between solutions processed with 'individual' and 'type mean' antenna calibration models. Two
790 instrumentation changes occurred at the station (marked by vertical dashed red lines): the first in
791 June 27th 2007, when the previous antenna was replaced with a TRM55971.00 and a TZGD
792 radome, and the second in June 28th 2013 with the installation of a TRM57971.00 and a TZGD
793 radome.Figure 3. EPN station KLOP (Kloppenheim, Frankfurt, Germany) ZTD differences time
794 series between solutions processed with 'individual' and 'type mean' antenna calibration models.
795 Two instrumentation changes occurred at the station (marked by vertical dashed red lines): the first
796 in June 27th 2007, when the previous antenna was replaced with a TRM55971.00 and a TZGD
797 radome, and the second in June 28th 2013 with the installation of a TRM57971.00 and a TZGD
798 radome.

799 Figure 4. Left part: Time series of the ZTD and up component differences between two time series
800 obtained with and without non-tidal atmospheric loading for two EPN stations: KIRO (Kiruna,
801 Sweden) and RIGA (Riga, Latvia)Figure 4. Left part: Time series of the ZTD and up component
802 differences between two time series obtained with and without non tidal atmospheric loading for
803 two EPN stations: KIRO (Kiruna, Sweden) and RIGA (Riga, Latvia).

804 Figure 5: VENE (Venice, Italy) time series of ZTD biases and standard deviations for the three
805 contributing solutions AS0, GO4 and MU4 with respect to the combined solution for the period
806 July 21st, 1996 - July 28, 2007 (GPS weeks 0863-1437). GO0 and GO1 are not shown here, since
807 they are very close to GO4.Figure 5: VENE (Venice, Italy) time series of ZTD biases and standard
808 deviations for the three contributing solutions AS0, GO4 and MU4 with respect to the combined
809 solution for the period July 21st, 1996 - July 28, 2007 (GPS weeks 0863-1437). GO0 and GO1 are
810 not shown here, since they are very close to GO4.

811 Figure 6: Weekly mean ZTD biases (upper part) and standard deviations (lower part) of each
812 contributing solution w.r.t. the final EPN-Repro2 combination.Figure 6: Weekly mean ZTD biases
813 (upper part) and standard deviations (lower part) of each contributing solution w.r.t. the final EPN-
814 Repro2 combination.

815 Figure 7. Long term up component repeatability the final coordinates for all stations. The site
816 coordinate repeatability is used as an internal quality metric. Stations are sorted by name.Figure 7.
817 Long term up component repeatability the final coordinates for all stations. The site coordinate
818 repeatability is used as an internal quality metric. Stations are sorted by name.

Formattato: Colore carattere: Automatico

Formattato: Tipo di carattere: Non Corsivo, Colore
carattere: Automatico

Formattato: Colore carattere: Automatico, Non
eseguire controllo ortografia o grammatica

Formattato: Colore carattere: Automatico

Formattato: Tipo di carattere: Non Corsivo, Colore
carattere: Automatico, Controllo ortografia e
grammatica

Formattato: Colore carattere: Automatico

Formattato: Tipo di carattere: Non Corsivo

Formattato: Tipo di carattere: (asiatico) Times New
Roman, Colore carattere: Nero

Formattato: Non Apice / Pedice

Formattato: Non Apice / Pedice

Formattato: Colore carattere: Automatico

Formattato: Tipo di carattere: Non Corsivo, Colore
carattere: Automatico, Controllo ortografia e
grammatica

Formattato: Colore carattere: Automatico

Formattato: Colore carattere: Automatico, Inglese
(Regno Unito)

Formattato: Colore carattere: Automatico

Formattato: Tipo di carattere: Corsivo

Formattato: Tipo di carattere: Non Corsivo

Formattato: Non Apice / Pedice

Formattato: Tipo di carattere: Non Corsivo, Controllo
ortografia e grammatica

Formattato: Inglese (Regno Unito)

Formattato: Inglese (Regno Unito)

Formattato: Tipo di carattere: (asiatico) +Corpo
asiatico (PMingLiU), Colore carattere: Automatico,
Inglese (Regno Unito)

819 Figure 8 VENE (Venice Italy) time series of daily repeatability (for definition, see Figure. 7) in the
820 up component for the period July 21st, 1996 - July 28, 2007 (GPS weeks 0863-1437). Figure 8
821 VENE (Venice Italy) time series of daily repeatability (for definition, see Figure. 7) in the up
822 component for the period July 21st, 1996 - July 28, 2007 (GPS weeks 0863-1437).

823 Figure 9 EPN station CAGL (Cagliari, Sardinia Island, Italy). Upper part: Radiosondes (in red) and
824 GPS (in blue) ZTD time series. Lower part: ZTD differences, calculated as RS minus GPS. Figure 9
825 EPN station CAGL (Cagliari, Sardinia Island, Italy). Upper part: Radiosondes (in red) and GPS (in
826 blue) ZTD time series. Lower part: ZTD differences, calculated as RS minus GPS.

827 Figure 10: GPS minus RS ZTD biases for all GPS-RS station pairs. The error bar is the standard
828 deviation. Sites are sorted with increasing distances from the nearest radiosonde launch site. Figure
829 10: GPS minus RS ZTD biases for all GPS-RS station pairs. The error bar is the standard deviation.
830 Sites are sorted with increasing distances from the nearest radiosonde launch site.

831 Figure 11: Distributions of station mean ZTD biases (left) and standard deviations (right) of EPN-
832 Repro1 and Repro2 compared to ERA-Interim. Figure 11: Distributions of station mean ZTD biases
833 (left) and standard deviations (right) of EPN Repro1 and Repro2 compared to ERA-Interim.

834 Figure 12: Site-by-site ZTD improvements of EPN-Repro2 versus EPN-Repro1 compared to ERA-
835 Interim. Figure 12: Site by site ZTD improvements of EPN Repro2 versus EPN Repro1 compared to
836 ERA-Interim

837 Figure 13: Time series of monthly mean biases (lower part) and standard deviations (upper part) for
838 ZTD differences between EPN-Repro2 and ERA-Interim re-analysis (GPS minus ERA-interim).
839 Uncertainties are calculated over all stations. Figure 13: Time series of monthly mean biases (lower
840 part) and standard deviations (upper part) for ZTD differences between EPN-Repro2 and ERA-
841 Interim re-analysis (GPS minus ERA-interim). Uncertainties are calculated over all stations.

842 Figure 14: Geographical distribution of ZTD biases (left) and standard deviations (right) for EPN-
843 Repro2 compared to ERA-Interim. Figure 14: Geographical distribution of ZTD biases (left) and
844 standard deviations (right) for EPN Repro2 compared to ERA-Interim.

845 Figure 15: ZTD trend comparisons at five EPN stations for 5 different ZTD datasets. The error bars
846 are the formal errors of the estimated trend values. Figure 15: ZTD trend comparisons at five EPN
847 stations for 5 different ZTD datasets. The error bars are the formal errors of the estimated trend
848 values.

Formattato: Inglese (Regno Unito)

Formattato: Tipo di carattere: Non Corsivo, Inglese (Regno Unito), Controllo ortografia e grammatica

Formattato: Inglese (Regno Unito)

Formattato: Inglese (Regno Unito)

Formattato: Non Apice / Pedice

Formattato: Tipo di carattere: Non Corsivo, Controllo ortografia e grammatica

Formattato: Inglese (Regno Unito)

Formattato: Inglese (Stati Uniti)

Formattato: Inglese (Regno Unito)

Formattato: Tipo di carattere: Non Corsivo, Inglese (Regno Unito), Controllo ortografia e grammatica

Formattato: Inglese (Regno Unito)

Formattato: Tipo di carattere: Non Corsivo, Controllo ortografia e grammatica

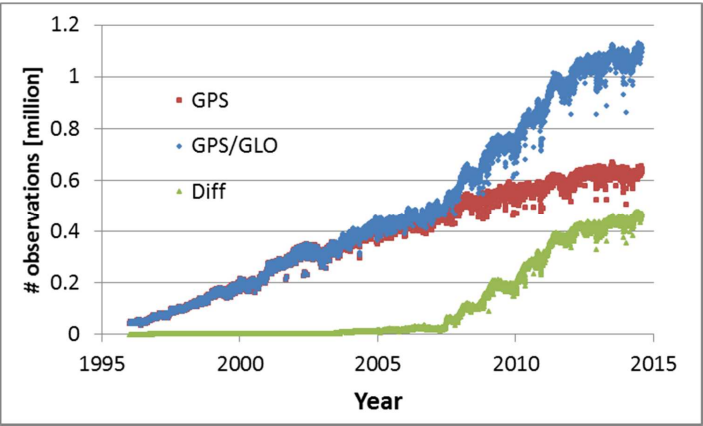
Formattato: Tipo di carattere: Non Corsivo, Controllo ortografia e grammatica

Formattato: Tipo di carattere: Non Corsivo, Controllo ortografia e grammatica

Formattato: Tipo di carattere: Non Corsivo, Controllo ortografia e grammatica

Formattato: Tipo di carattere: Non Corsivo, Controllo ortografia e grammatica

850



851

852 Figure 1. Time series of the number of GNSS observations for the period 1996-2014. GPS
853 observations are shown in red, GPS+GLONASS in blue and their differences in green. The
854 difference becomes significant starting from 2008.

855

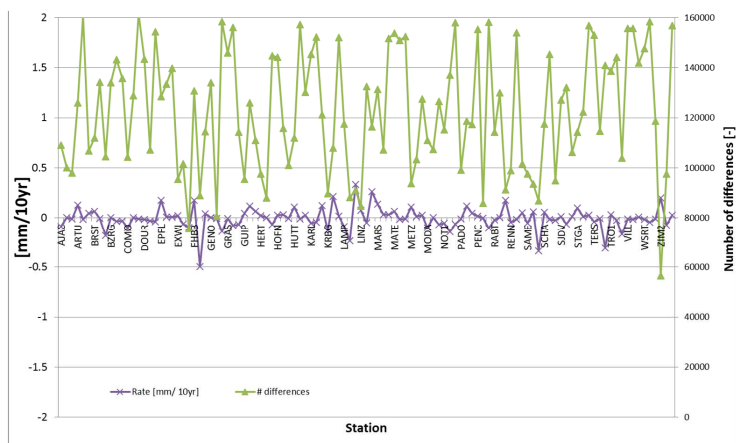


Figure 2. ZTD trend differences between GPS only and GPS+GLONASS, computed over 111 sites. The rate is in violet (primary y-axis) and the number of used differences is in green (secondary y-axis).

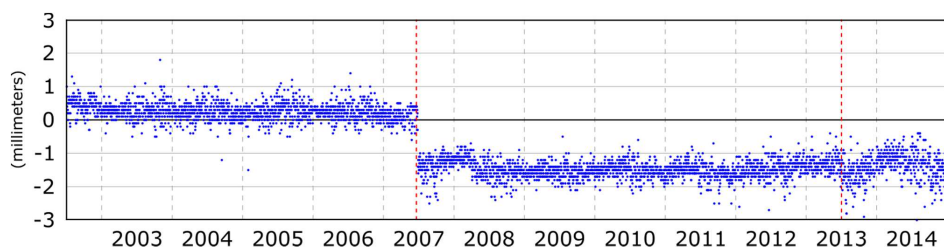


Figure 3. EPN station KLOP (Kloppenheim, Frankfurt, Germany) ZTD differences time series between solutions processed with ‘individual’ and ‘type mean’ antenna calibration models. Two instrumentation changes occurred at the station (marked by vertical dashed red lines): the first in June 27th 2007, when the previous antenna was replaced with a TRM55971.00 and a TZGD radome, and the second in June 28th 2013 with the installation of a TRM57971.00 and a TZGD radome.

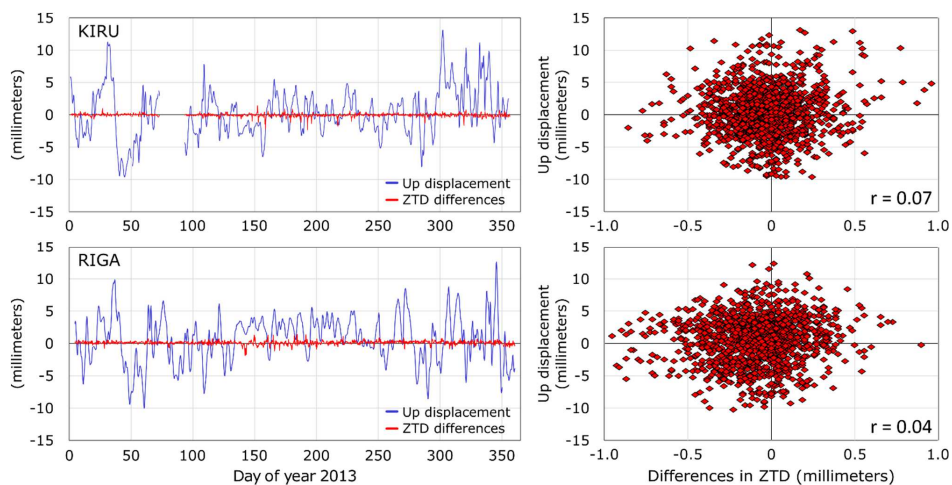
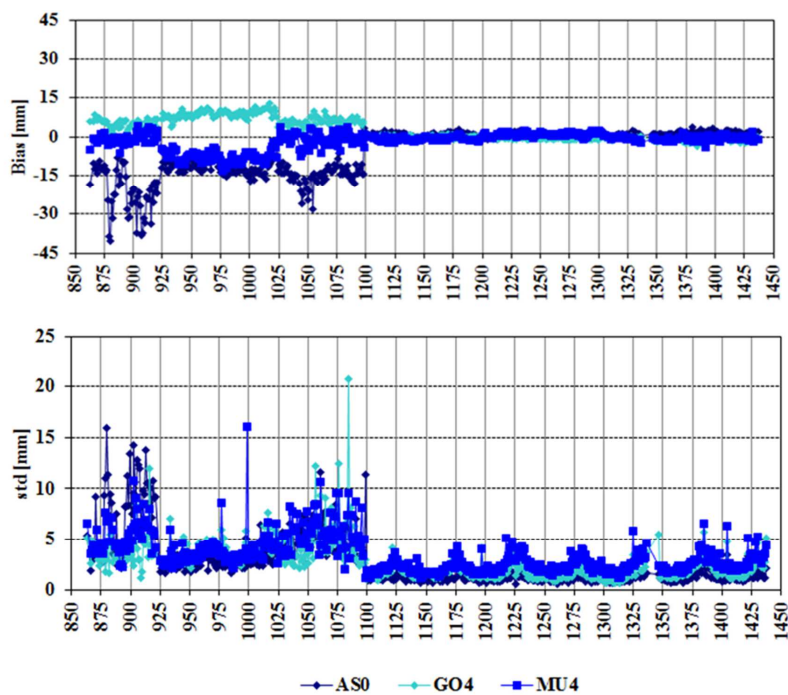


Figure 4. Left part: Time series of the ZTD and up component differences between two time series obtained with and without non-tidal atmospheric loading for two EPN stations: KIRO (Kiruna, Sweden) and RIGA (Riga, Latvia). Right part: Scatter plots between these two parameters.



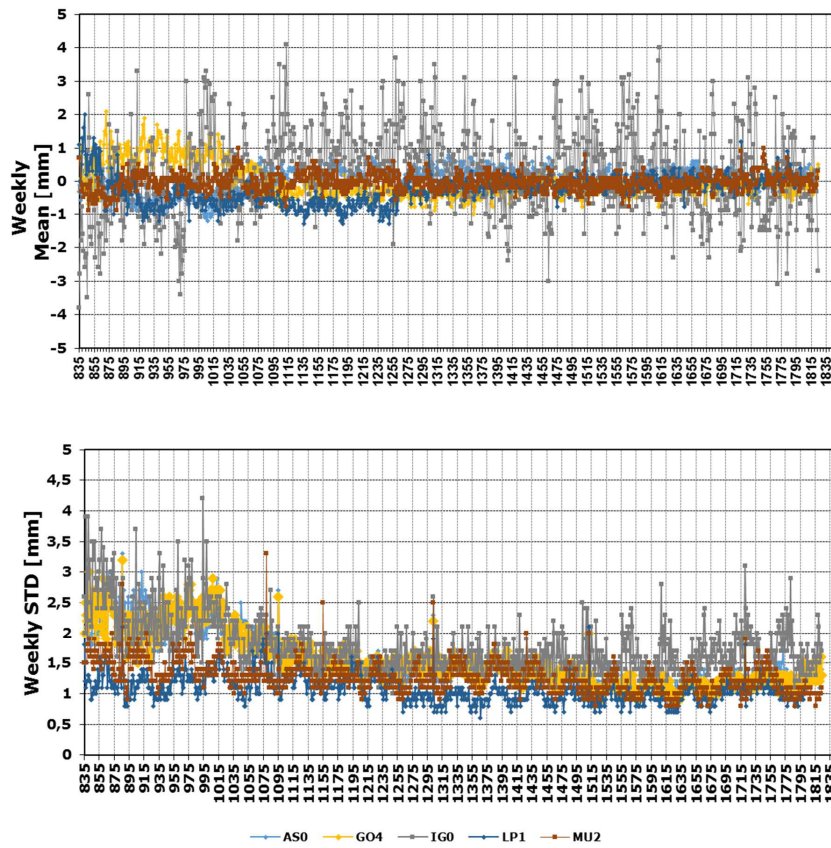
873

874 Figure 5: VENE (Venice, Italy) time series of ZTD biases and standard deviations for the three
 875 contributing solutions AS0, GO4 and MU4 with respect to the combined solution for the period
 876 July 21st, 1996 - July 28, 2007 (GPS weeks 0863-1437). GO0 and GO1 are not shown here, since
 877 they are very close to GO4.

878

Commentato [RVM52]: I assume?

Commentato [PR53R52]: yes



879
 880 Figure 6: Weekly mean ZTD biases (upper part) and standard deviations (lower part) of each
 881 contributing solution w.r.t. the final EPN-Repro2 combination.
 882

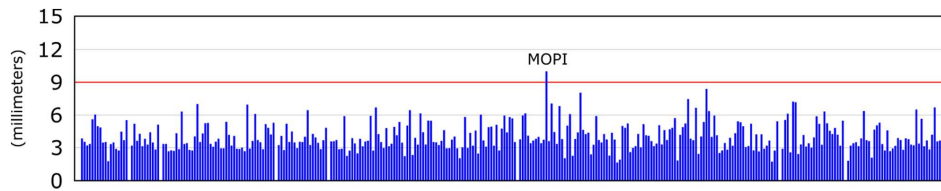


Figure 7. Long term up component repeatability the final coordinates for all stations. The site coordinate repeatability is used as an internal quality metric. Stations are sorted by name.

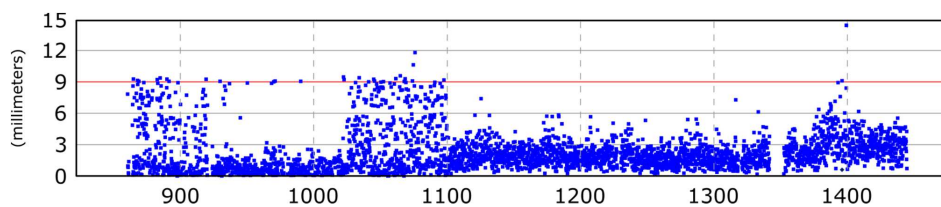
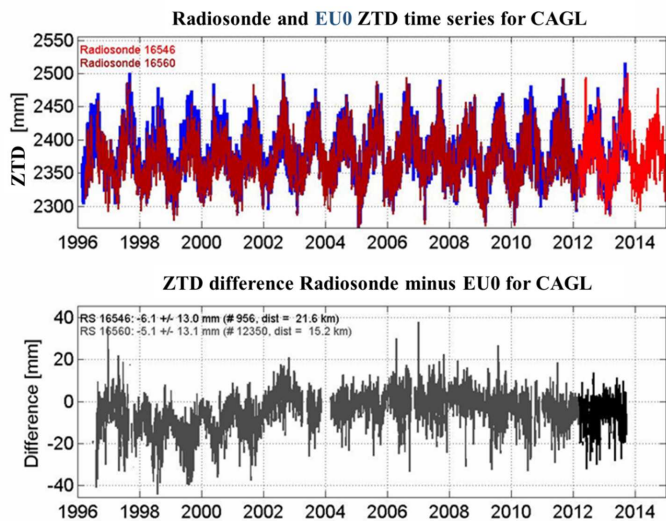


Figure 8 VENE (Venice Italy) time series of daily repeatability (for definition, see Figure. 7) in the up component for the period July 21st, 1996 - July 28, 2007 (GPS weeks 0863-1437).

891



892

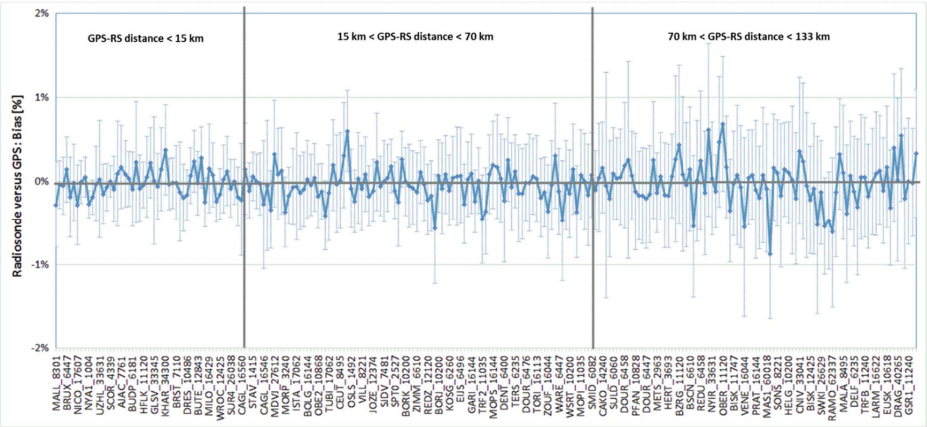
893 Figure 9 EPN station CAGL (Cagliari, Sardinia Island, Italy). Upper part: Radiosondes (in red) and
894 GPS (in blue) ZTD time series. Lower part: ZTD differences, calculated as RS minus GPS.

895

Commentato [g54]: In this figure, you use ZPD instead of ZTD. You do not explain what it stands for and this is also very inconsistent with the rest of the paper. Please change the titles and the label in the figure!

Commentato [PR55R54]: Done

896



897

898 Figure 10: GPS minus RS ZTD biases for all GPS-RS station pairs. The error bar is the standard
899 deviation. Sites are sorted with increasing distances from the nearest radiosonde launch site. The x-
900 axis shows the GPS station and the radiosonde site WMO code.

901

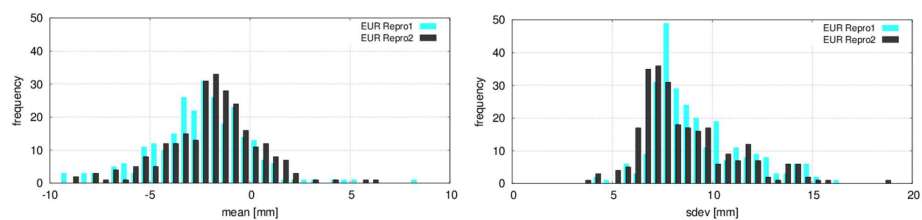
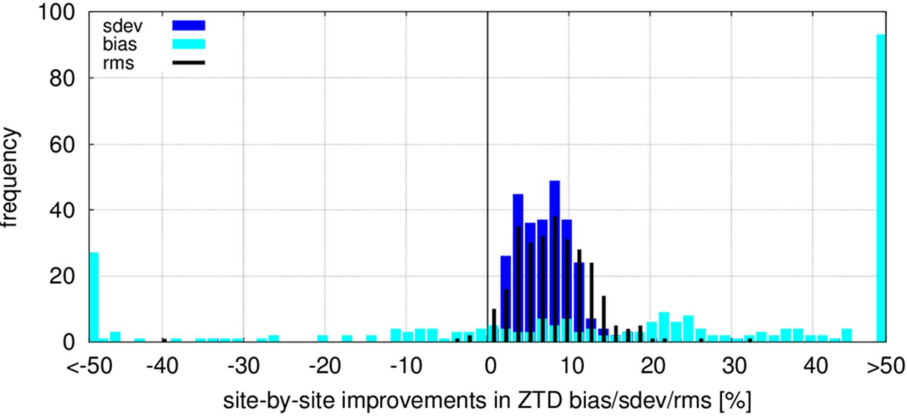


Figure 11: Distributions of station mean ZTD biases (left) and standard deviations (right) of EPN-Repro1 and Repro2 compared to ERA-Interim.

906

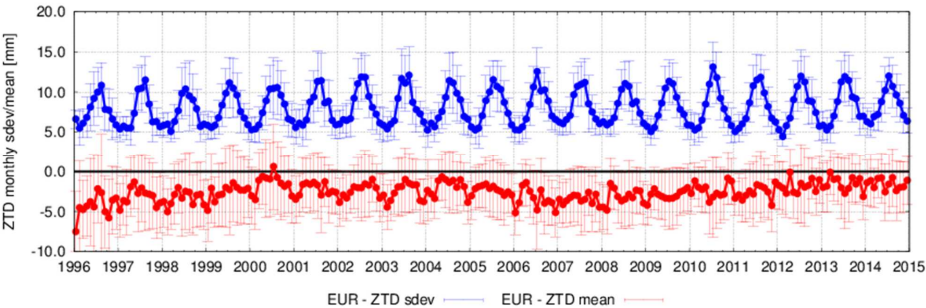


907

908 Figure 12: Site-by-site ZTD improvements of EPN-Repro2 versus EPN-Repro1 compared to ERA-
909 Interim.

910

911



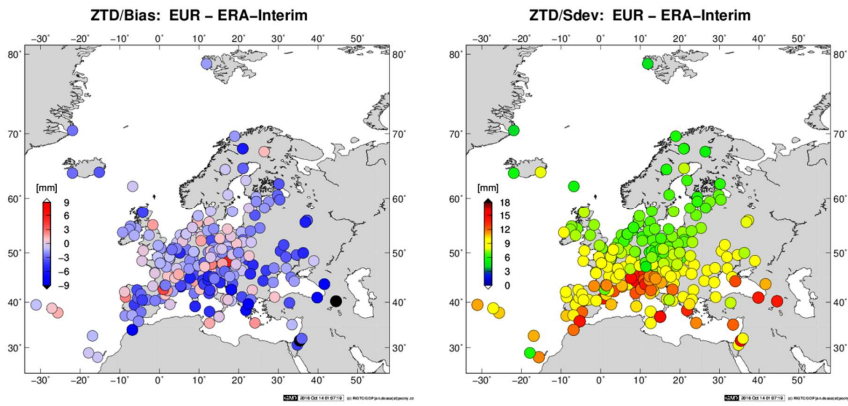
912

913 Figure 13: Time series of monthly mean biases (lower part) and standard deviations (upper part) for
914 ZTD differences between EPN-Repro2 and ERA-Interim re-analysis (GPS minus ERA-interim).
915 Uncertainties are calculated over all stations.

916

Commentato [RVM56]: Please confirm or modify.

Commentato [PR57R56]: yes



917

918 Figure 14: Geographical distribution of ZTD biases (left) and standard deviations (right) for EPN-
 919 Repro2 compared to ERA-Interim.

920

921

922

923

924

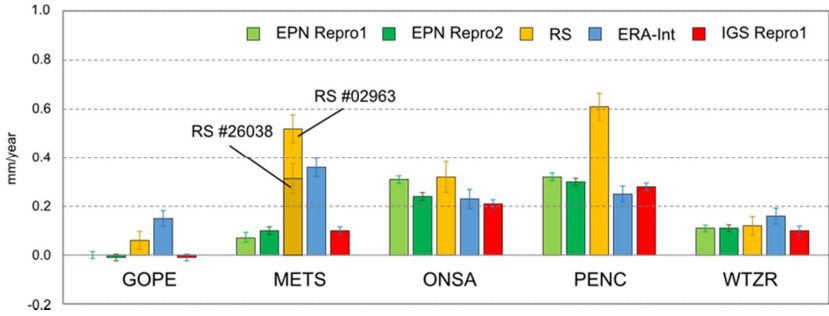


Figure 15: ZTD trend comparisons at five EPN stations for 5 different ZTD datasets. The error bars are the formal errors of the estimated trend values.